**TECHNISCHE
UNIVERSITÄT
ILMENAU**

PUCP

Mechanical bearings with tunable compliance after biological role
model of blood sinus hairs

Bachelor: Jorge Luis Ingaroca Quispe

Thesis submitted for the degree of
Master of Science in Mechatronics
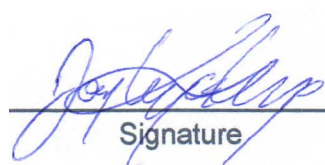
Advisors, Ilmenau:
Dipl.-Ing. Thomas Helbig

Advisors, Lima:
Dr. Ing. Jorge Alencastre

Supervising Professor, Ilmenau:
Univ.-Prof. Dipl.-Ing. Dr. Med.(habil.) Hartmut Witte

Ilmenau – Germany
2016

Hereby, I declare that I have elaborated the present work without any non-specified assistance. The people involved in the research, literature, as well as any another resource used in this thesis, has been completely specified throughout and the end of the text.

26th April 2016, Ilmenau.

_____
Signature

Abstract

In follicle sinus complex of sinus hairs, two blood vessels seem to have a prominent function. Up to date, their biological role is unknown, however, hypothesis suggest that they are used as hydraulical bearing for the hair which is used to change the stiffness and compliance of the fixation depending on the application. Because of the size of the structures of interest experiments at the living object to clarify the biological role are not possible so far. Therefore, mechatronic approaches can help to investigate advantages and possibilities of a bearing with tunable compliance. Thus, in the current thesis, it is develop a mathematical modeling, multi-body simulation and a mechatronic demonstrator of a swinging rod in a bearing with tunable compliance. The tunable compliance of the system was inspired of Jack Spring principle of work, which change the compliance by decreasing the number of active coils.

Acknowledgment

I would like to express my gratitude to my advisor in TU-Ilmenau, Dipl.-Ing. Thomas Helbig, for his immense support and advices during the develop of this thesis.

My sincere thanks to Professor Witte, for allowing me to work in this thesis theme of the Department of Biomechatronic Engineering.

I appreciate the patience and support of Professors Dr. Ing. Jorge Alencastre and Dr. Ing. Julio Tafur, from PUCP, during the development of this current thesis.

I would also like to express my gratitude to my family who supported me and always believes in me, even before I do myself. A whole year far from them made me realize I love them much more than I ever thought.

I would like to thank to my friends who accompanied me in this experience. Their support was fundamental in this last section.

Finally, but not less important, I would like to express my gratitude to all the people who always cared of me, with a call, a message, supporting words or being with me in this stage of my life.

Contents

1 Introduction

1.1 Motivation

Nature, in its wise development, provided living beings with characteristic that made them possible to survive and adapt to the conditions of their environment. There are several differences among the characteristics of all the species of the world. Most of those characteristics that living beings own, are still unknown for humans; however, the understanding of the biological characteristics of the creatures in nature could open multiple possibilities to be employ to solve problems update without solutions or improve them with new advantages. In this context, many researches focused on rats and their abilities such as nocturnal rodents to perform their locomotion with high precision. These studies give some evidences that rats use a complex method of detection surface and objects by using their vibrissa. The State of the are about vibrissa and Follicle-sinus complex provides information about how biological mechanism inside the follicle-sinus complex might change viscoelastic properties in order to switch operating modes. This variation of viscoelastic properties, hypothetically is achieved by adjusting the flow of blood in the blood vessel inside the follicle-sinux complex. Here, the concept of tunable compliance owns a great meaning. The idea of tunable compliance has a prominent future in many fields of engineering. This ability to varying the viscoelastic properties of an actuator would mean a higher energy efficiency. For example, in rehabilitation, prosthesis and walking biped robot, actuators with tunable compliance improve their developments. There have been many researches about actuators with tunable compliance, and had reached good results to be employ in robotics. Besides, for control systems, it can be long employed to change parameter that are not common to be tuned, providing robustness to the system. In summarize, compliant actuators have a great potential for applications in mechatronics.

2 Biological paradigm

2.1 Vibrissa

The vibrissa are sinus hairs that are commonly found in rats, cats, seals and rodents. These sinus hairs provide them special skills not only for social interaction with their own kind, but for grasping activities that involves the control of their locomotion ([KKL$^+$10],[Bed00]). In the case of marine mammals, vibrissae is useful to detect pressure changes [MAKL06]. Rats are known as nocturnal rodents, since their vibrissa offer them detection of environment characteristics as a non-visual sensory system. It is important to remark that vibrissa features, e.g. number, geometric arrangement, size, morphology, shape and stiffness, vary among animals [GDFM12].

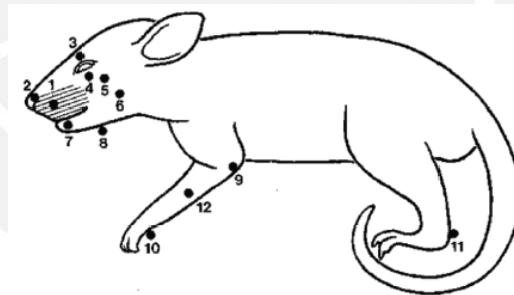Figure 2.1: Vibrissae classification according of its location [Car10] (1)mystacial (2)rhinal (3)supraorbital (4)infraorbital (5)postorbital (6)buccal (7)mystacial (8)interramal (9)anconeal (10)ulnar carpal (11)calcaneal (12)medial antebrachial

In figure 2.1, it can be seen the different types of vibrissa that exists according to its location on rats body. Also, according to its position has a position relationship and
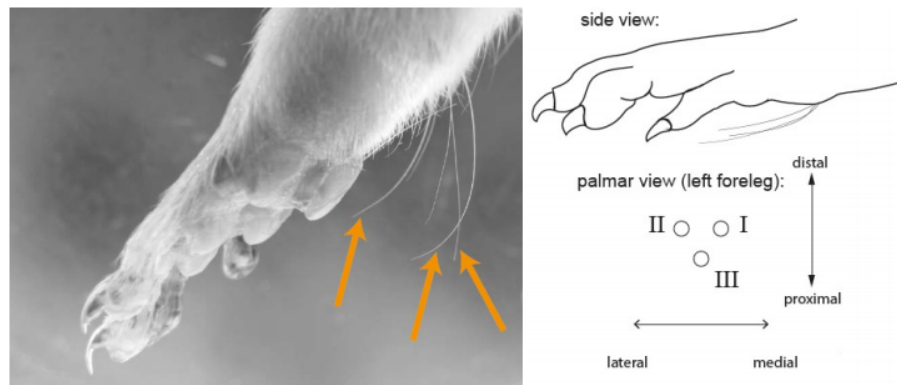
numbering, as it can be viewed in 2.2.

Figure 2.2: Position relation and numbering of carpal Vibrissa [SWZ⁺14]

Up to date, there are more knowledges about structure and function of mystacial sinus hair than carpal sinus hair. However, lately, carpal sinus hairs have gained interest because there are researches that evidence its influence in kinematics of rat legs ([HVN⁺14b], [BSWZ13], [Dör82]). Hypothesis, also suggest that carpal sinus hair is used to vary the stiffness in the follicle-sinus complex of the legs in order to prepare them for contact with substrate ([BSWZ13], [HVN⁺14b]). In the whole structure of vibrissa, there is not any receptor to transmit the external information (external forces) because it is composed by a dead material [BSWZ13]. Thus, the mechanoreceptors in the follicle-sinus complex, as it can be seen in figure 2.5, make possible the detection when they suffer a pressure mechanically transmitted by the vibrissa. The number of mechanoreceptors between mystacial and carpal sinus hairs are different, so it is understood that they have different functions ([FAR95], [EKM⁺02]). FUNDIN ([FAR95]) explains that carpal sinus hairs have an importance in activities such as eating and grasping or also in detection of vibrations of the ground. There are also hypothesis about its influence in locomotion and kinematics of rat legs. Researches made in [NWS15] and [HVN⁺14a] demonstrate that movements of rat vary when they walk without carpal sinus hairs. Therefore, carpal sinus hairs might have a function for locomotion. The mystacial sinus hair detects vertical obstacles and can measure the spatial body position [SWZ⁺14]. Consequently, there should be another sensor to guarantee the skill of recognizing obstacles and substrate composition in order to stabilize the body position [SWZ⁺14]. This is why carpal sinus hairs is

supposed to recognize irregular substrate when touchdown occurs [HVN$^+$14a]. Carpal sinus hairs has different characteristics than mystacial sinus hairs such as length and curved shape. Because the position of forelimbs is important to stabilize locomotion, carpal sinus hairs might have a prominent function to detect horizontal changes in surface ([HVN$^+$14a], [SWZ$^+$14]). BERG and KLEINFELD distinguished two whisker patterns in rats: exploratory whisking, when rats explore the environment sweeping their whiskers with high amplitude and low frequency (5-15 Hz); and foveal whisking, when rats contact surface of objects with small amplitude and high frequency (15-25 Hz) [BK03].

2.2 Follicle-sinus Complex

The tactile signals are transmitted by the vibrissae to the receptors in Follicle-sinus Complex. The Follicle-sinus complex (FSC) is a sensory receptor located in the root of vibrissae; which supports the sinus hair and contains many components that allow the detection of force signals ([Car10], [SWZ$^+$14], [HVN$^+$14a], [BSWZ13]). The FSC is composed by vibrissal shaft and a follicle which has an outer root sheath surrounded by a glassy membrane ([KKL$^+$10], [FAR95]). The blood sinus encloses the follicle. The blood sinus is divided by two parts; a superior part, named Ring sinus, and a inferior part, named Cavernous sinus ([Fli14], [BSWZ13], [Car10]). In the ring sinus, there is a C-shaped Ringwulst. A collagenous capsule encloses the vibrissal shaft and blood sinus, until the neck of the follicle creating an outer and inner conical body [KKL$^+$10]. In the cavernous sinus, the superior part has less blood than the inferior one. The Follicle-sinus complex has an important function because amplifies the movement of the vibrissae, so the mechanoreceptors located at the base of vibrissa can detect small stimuli [KKL$^+$10].
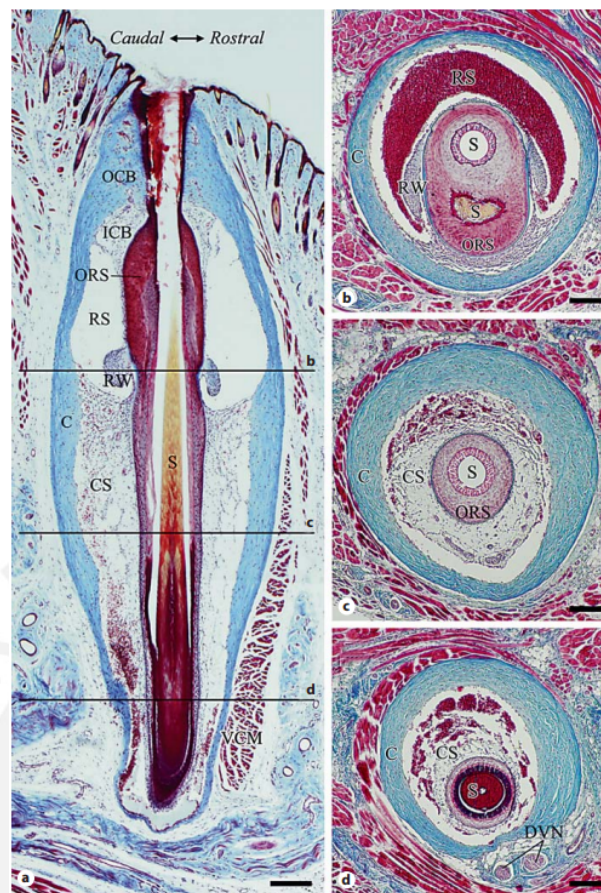
Figure 2.3: Histology of vibrissal Follicle-sinus complex [KKL$^+$10]. (a) Sagittal section of Follicle-sinus complex (b)Transverse section of ring sinus and ringwulst (c) Transverse section of carvernous sinus (d) Transverse section of cavernous sinus in the lower level. C=Collagenous capsule; CS=Cavernous sinus; DVN=Deep vibrissal nerve; ICB=Inner conical body; OCB=Outer conical body; ORS=Outer root sheath; RS=Ring sinus; RW=Ringwulst; S=Vibrissal shaft; VCM=vibrissal capsular muscle

The FSC and the muscle system allow rodents to use their vibrissa in two modes of operation: Passive mode, and Active mode. In passive mode, when the vibrissa is deflected by external forces and return passively into its initial position. In active mode, vibrissa is swung by contractions of intrinsic an extrinsic muscles ([BSWZ13], behn2009finite). The figure 2.4 shows a schematic drawing of FSC where there are intrinsic and extrinsic muscles. So, triggering oscillations with different frequencies and amplitudes, rodents are able to investigate objects and its characteristics, such

as shape and surface, in a quickly way. Hitherto, the way they can convert that information of their surroundings is still unknown [BSWZ13].
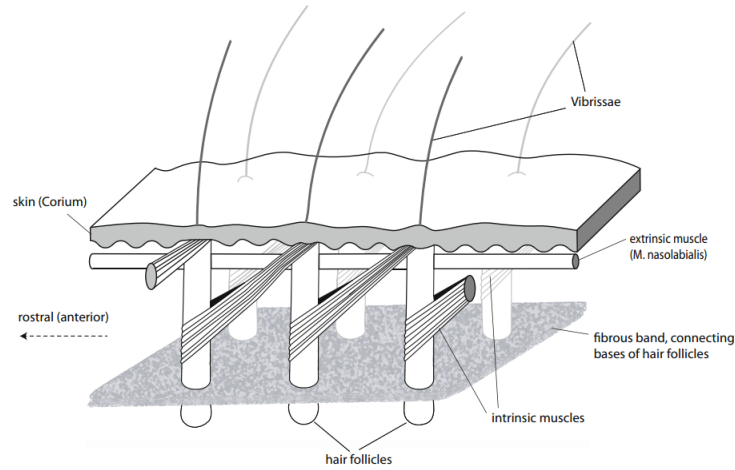

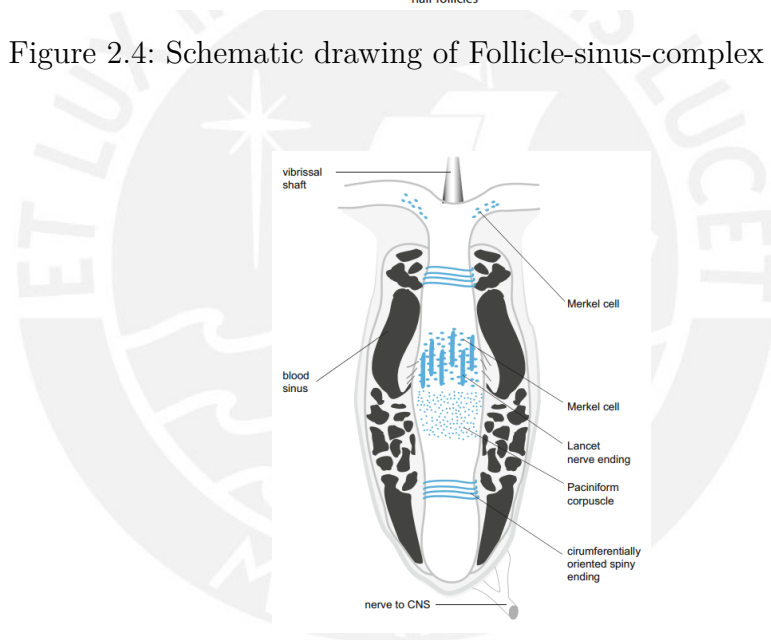Figure 2.4: Schematic drawing of Follicle-sinus-complex [BSWZ13]

Figure 2.5: FSC ofa vibrissa with different receptors (blue) [BSWZ13]

Theory suggest that probably rodent can adjust the stiffness of the support in the vibrissa by varying the flow of blood in the ring sinus, so it changes the pressure in the blood-sinus and, of course, its viscoelastic properties [Dör82].

3 State of the art

3.1 Mechanical models of Follicle-sinus complex

Because the mechanical behaviour of the FSC might be significant in the development of autonomous robots, there have been researches trying to identify the mechanical parameters involve on it in order to study the dynamical behaviour of vibrissa [BSWZ13]. Usually, the models used are rigid body models and continuum models. In [MGR+04], researches create an electro-mechanical model of rat mystacial Follicle-Sinus complex in order to give a clearer idea about the transduction process to recognize the information of force given by vibrissa to its Follicle-sinus complex.
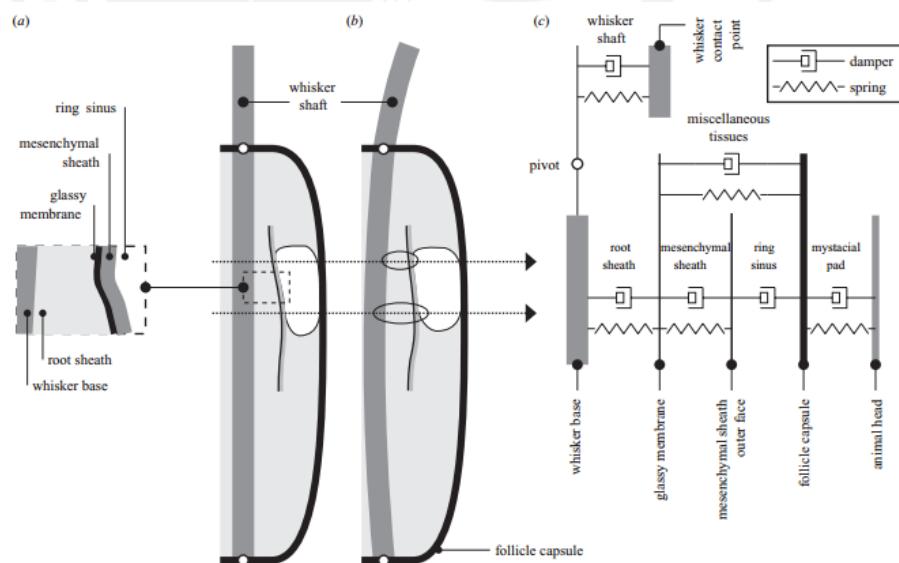
Figure 3.1: (a)Simplify FSC anatomy (b)effect of deflection and (c)exploded FSC mechanical model [MGR+04]

The biological elements involve in the follicle are represented by dampers and springs. There are also researches focussing on the relationship among the muscles associated in vibrissae motion [HBZK08]. To achieve that, three follicles are linked by dampers and springs among them in order to represent the influence of intrinsic muscle in the other follicles.

Another approach is presented in [BK03], where the passive elements used in the mechanical model of whisker represents the components in the FSC such as skin, plate, and intrinsic and extrinsic muscles as it is shown in figure 2.4.
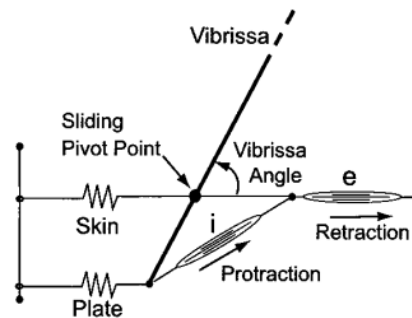
Figure 3.2: Model of mystacial vibrissae regarding components such skin, plate, and intrinsic and extrinsic muscles [BK03]
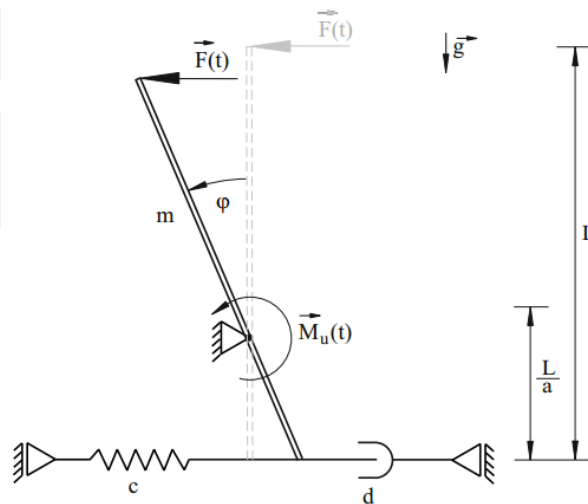
Figure 3.3: Model of a rod-like vibrissa of 1 DoF. Where $M_U(t)$ represents the torque produced by rodents in their vibrissae to use it in active mode [BSWZ13]
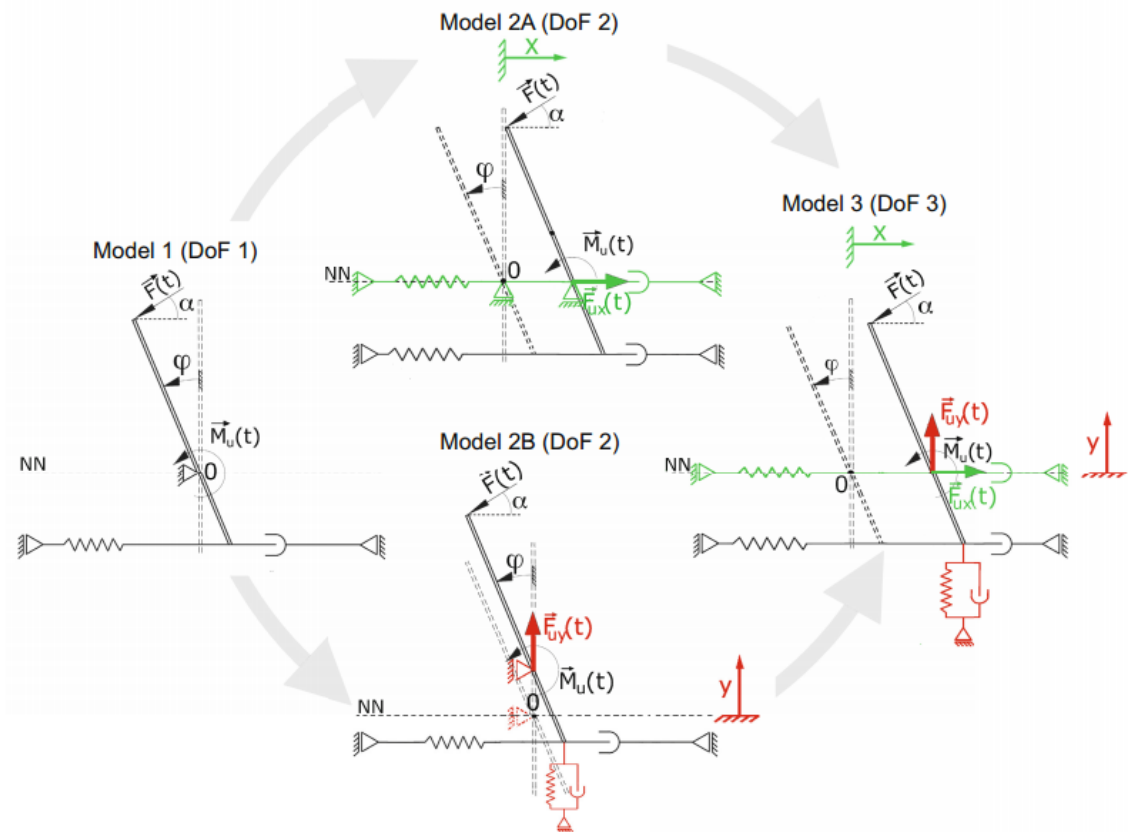
Figure 3.4: Model with multiple degrees of freedom [BSWZ13]

However, to achieve a better accuracy of the mechanical system involve in the FSC of a vibrissa, the higher quantity of elements in the FSC should be represented. In figure 3.5 a complex vibrissae model is shown with multiple springs and dampers. In this model, the viscoelastic properties of the blood-sinus are represented by compliant elements (spring and damper) [SSWB11].
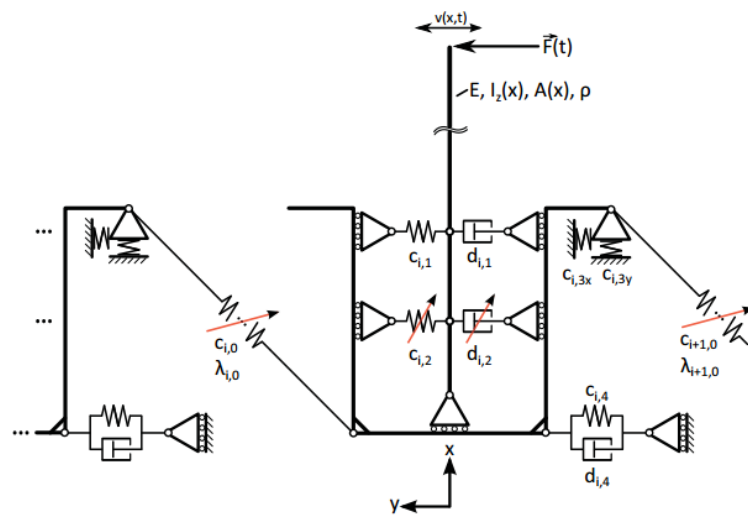
Fig. 5. Example of a vibrissa model

Figure 3.5: Complex model of vibrissae in the mystacial pad [SSWB11]

3.2 Actuator with adaptable compliance

In the growing fields of wearable robotics, rehabilitation robotics, prosthetics, and walking robots, actuators with adjustable compliance have gained a great importance due to its ability to minimize large forces produced by shocks, to interact safely with users, and to store and then release energy in passive elastic elements [HSV+09]. In classic robotic, the actuators are desired to be as stiff as possible in order to reach accurate positions or trajectories. However, mechanically, muscle has a great potential because of its superior functional performance and control system with the advantage of tunable parameters ([VHVVD+07], [HSV+09]). It is important to notice that systems with tunable compliance has less accuracy than stiff actuators. There are two groups of applications that require system with adaptable compliance: Robot-human interaction and for adjusting natural dynamics [HSV+09].

Robot-human interaction
In this first group, it is required to guarantee a safety and natural interaction between robot and user. For instance, in industrial robots, the actuator are really stiff, and do not relief the damage produced by shocks or collisions. It is not a big deal while

working in human-free environment. However, for application where exists interaction with humans, it is needed to work with safer robots [ZKRS04]. In that case, the actuator would act with a predefined stiffness when it is required to operate with precise positioning, and compliant when it requires higher speeds. For rehabilitation, as well, is required the dissipation of undesired movements. For example in the case of patients who suffer spasms, stiff actuators could damage their legs. Thus, actuators with tunable compliance would reduce those errors preventing the damage to the system and the user. Besides, at the beginning of rehabilitation process, it is desired a low stiffness; however according to the progress of the patient by using the system, it will be necessary a higher stiffness ([VHVVD+07], [HSV+09]).

Adjustment of natural dynamics In this group, it is required the adjustment of the compliance of an actuator in order to change the natural motion into a desired motion. It is applicable in fields of robotic prosthesis, where is required and adjustment of the stiffness in actuators to enhance the comfort for user. Thus, by using stiff actuator, the stiffness is fixed and would work just for certain applications. For instance, in transtibial prosthesis [HSV+09], with a fixed stiffness will operate comfortably for user but just for certain type of surface. Therefore, the ability of tuning the stiffness would optimize the behaviour of the system. As well, for walking biped robots, tunable compliance of actuator would upgrade the amount of energy because it could be stored during the touchdown and then released during push-off [HSV+09]. Also, by varying the stiffness, the frequency of the system is adjusted allowing the system to walk slower or faster.

To achieve energy storage as well as adaptable compliance, it is required an elastic element. Many researches has presented novel design to reach these objectives.
In figure 3.6, the principle of work of MACCEPA is shown. MACCEPA is a novel compliant system. The compliance is achieved by pre-stretching the spring with a servomotor, so it would change the response and frequency of the joint. This is a novel compliant actuator that have won great importance because of its simplicity.
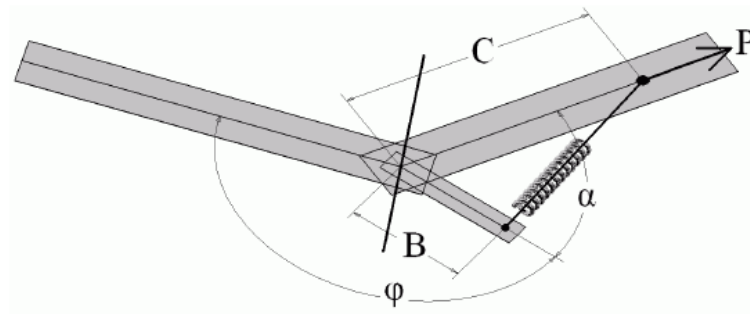
Figure 3.6: Working principle of MACCEPA [VHVVD$^+$07]

In figure 3.7, the Jack spring actuator has an interesting manner to change the stiffness by varying the number of active coils of the spring. It is because the stiffness of the spring depends on some parameters such as wire coil, wire diameter, modulus of rigidity, and number of active coils. Because modifying the values of the other parameters is not that simple, it focuses on varying the number of active coils. Number of active coils are inversely proportional to stiffness.
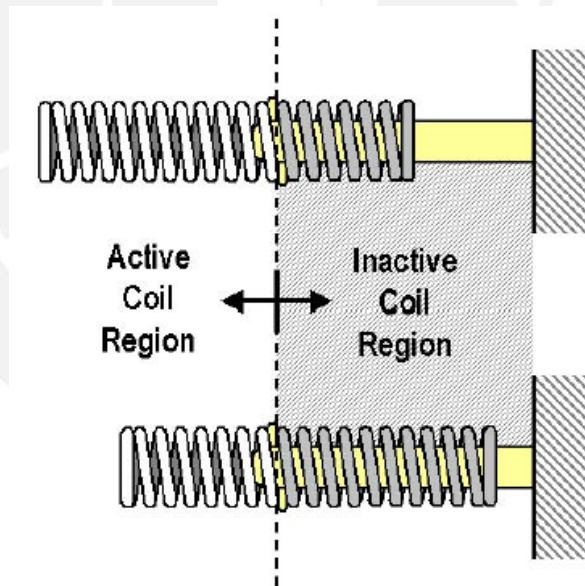
Figure 3.7: Concept of 'Jack Spring' [HSH05]

In figure 3.8, it can be seen an actuator with two extensions springs that provide the compliance, both springs are linked to an element controlled by a motor. In order to

safe space, a spring steel wire was also used as a replacement of extension springs.
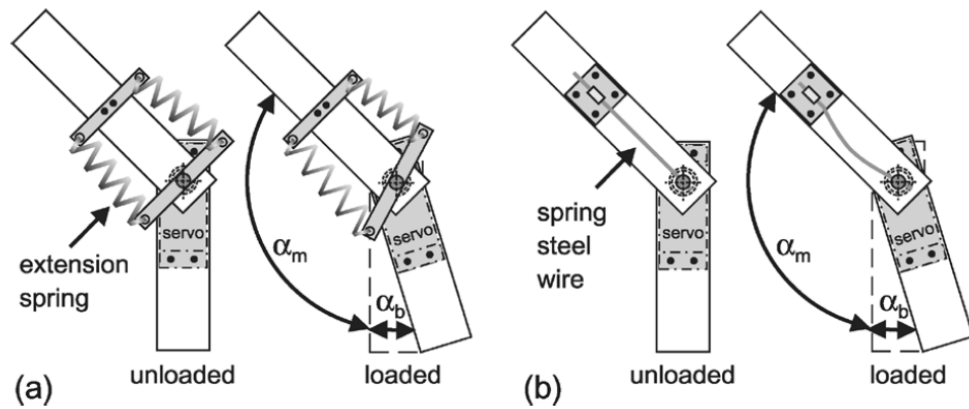
Figure 3.8: Model proposed in [SCS05]. (a)Extension springs used to generate the compliance in the actuator (b)Instead of extension springs, a single steel wire is used to save space

4 Theoretical foundation

4.1 Vibrations and damping

The interest of the study of vibrations comes from ancient times where the first musical instruments were created. In their study they have involved great personages of science as Pythagoras, Hooke, Galileo. The phenomenon of mechanical vibrations has been part of the considerations on mechanical structures because it improves their designs and prevent the collapse of these, as is in the case of the effects of resonance frequency.

Vibrations or oscillations are movements that are repeated in a time interval around a stable equilibrium position. A vibrating system contains three components. The first one transfer potential energy. The second one stores the potential energy as kinetic energy. And the third one is that dissipates the energy of the system. Therefore, in a vibration exists an alternating transfer of kinetic energy to potential, and in some cases contain an energy dissipater element. Mechanical vibrations can be classified in multiple ways.

**Free and forced vibrations**
Free vibrations are those in which only inherent forces to the system elements act in vibration. In other words, it does not use any external force on the system. In contrast, the forced vibrations are those where exists one or more external forces acting on the vibration. At this point it is important to remember that if the frequency of the external force is equal to the natural frequency of the system, the system goes into resonance which is subjected to very large swings that could bring down the system.

Damped and undamped vibrations

If there is no loss of energy in the oscillations of a vibration, it would be a case of undamped vibration. Then, in vibrations where their oscillations amplitude decreases in each swing, they are called damped vibrations.

Linear and non-linear vibrations

If the components of a vibratory system have linear behavior, then we say that the system results in a linear vibration. Conversely, if the components of a mechanic vibration are non-linear, it implies that the vibration will be non-linear.

Then it may be the case where there is free or forced vibration damped and non-damped. For the current thesis, theoretical behaviour of free damped vibrations will be described.

The figure represents a mass-spring-damper system which is a system with simple harmonic motion movement and damping.
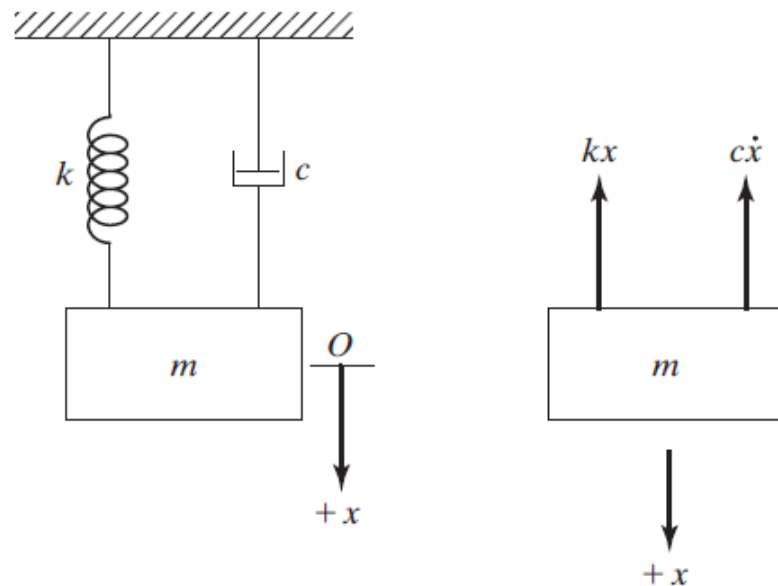
Figure 4.1: Mass-spring-damper system [RY95]

In the equation 4.1, it is described the equation of forces.

$$m\ddot{x} + c\dot{x} + kx = 0 \tag{4.1}$$

Where:

m: represents the mass of the block

k: stiffness of the spring

c: damper of the system

To solve equation 4.1, we assume as a solution:

$$x(t) = Ce^{st} \tag{4.2}$$

Where C and s are undetermined constants. So, if we replace in the equation 4.1 the next equation is obtained:

$$ms^2 + cs + k = 0 \tag{4.3}$$

Then, from equation 4.3 we obtain the following roots:

$$s_{1,2} = \frac{-c \pm \sqrt{c^2 - 4mk}}{2m} = -\frac{c}{2m} \pm \sqrt{\left(\frac{c}{2m}\right)^2 - \frac{k}{m}} \tag{4.4}$$

$$x(t) = C_1 e^{\left(-\frac{c}{2m} + \sqrt{\left(\frac{c}{2m}\right)^2 - \frac{k}{m}}\right)t} + C_2 e^{\left(-\frac{c}{2m} - \sqrt{\left(\frac{c}{2m}\right)^2 - \frac{k}{m}}\right)t} \tag{4.5}$$

The values of constants C_1 and C_2 are constants determined from initial conditions

4.1.1 Case 1: Under-damped system

This case occurs when it satisfies this situation:

$$\frac{c}{2m} < \sqrt{\frac{k}{m}} \tag{4.6}$$

In this case the roots are complex and the response will result:

$$x(t) = C_1 e^{\left(-\frac{c}{2m} + i\sqrt{\frac{k}{m} - \left(\frac{c}{2m}\right)^2}\right)t} + C_2 e^{\left(-\frac{c}{2m} - i\sqrt{\frac{k}{m} - \left(\frac{c}{2m}\right)^2}\right)t} \tag{4.7}$$

Then:

$$x(t) = e^{-\frac{c}{2m}t} \left\{ (C_1 + C_2) \cos\left(t\sqrt{\frac{k}{m} - \left(\frac{c}{2m}\right)^2}\right) + i\left(C_1 - C_2\right) \sin\left(t\sqrt{\frac{k}{m} - \left(\frac{c}{2m}\right)^2}\right) \right\} \tag{4.8}$$

$$x(t) = X e^{-\frac{c}{2m}t} \cos\left(\left(\sqrt{\frac{k}{m} - \left(\frac{c}{2m}\right)^2}\right)t + \Phi\right) \tag{4.9}$$

Where X and Φ can be obtained from initial conditions.

Thus, from equation 4.9, it can be predicted that its response will be periodic with a tendency to decrease to zero. These vibrations are called under-damped vibrations.

4.1.2 Case 2: Critically damped system

It occurs when the following is true:

$$\frac{c}{2m} = \sqrt{\frac{k}{m}} \tag{4.10}$$

Therefore, the roots are purely real.

$$s_1 = s_2 = \sqrt{\frac{k}{m}} \tag{4.11}$$

Then, a solution for the response is given for the next equation:

$$x(t) = (C_1 + C_2 t) \, e^{-\frac{c}{2m} t} \tag{4.12}$$

Because of the effect of exponential function the response of this system will be non-periodic with a tendency of decrease rapidly to zero.

4.1.3 Case 3: Overdamped system

This system occurs when:

$$\frac{c}{2m} > \sqrt{\frac{k}{m}} \tag{4.13}$$

So, the roots are real but distinct and are given by:

$$s_1 = -\frac{c}{2m} + \sqrt{\left(\frac{c}{2m}\right)^2 - \frac{k}{m}} \tag{4.14}$$

$$s_2 = -\frac{c}{2m} - \sqrt{\left(\frac{c}{2m}\right)^2 - \frac{k}{m}} \tag{4.15}$$

Where $s_1 \ll s_2$, and the response of this system would be given by:

$$x(t) = e^{-\frac{c}{2m}} \left\{ C_1 e^{\left(\sqrt{\left(\frac{c}{2m}\right)^2 - \frac{k}{m}}\right) t} + C_2 e^{\left(-\sqrt{\left(\frac{c}{2m}\right)^2 - \frac{k}{m}}\right) t} \right\} \tag{4.16}$$

The response of the system would be non-periodic. However, it decreases slowly to zero.
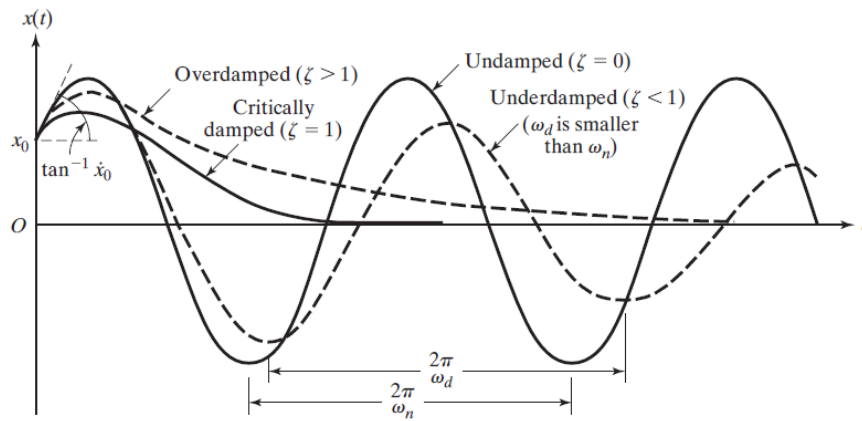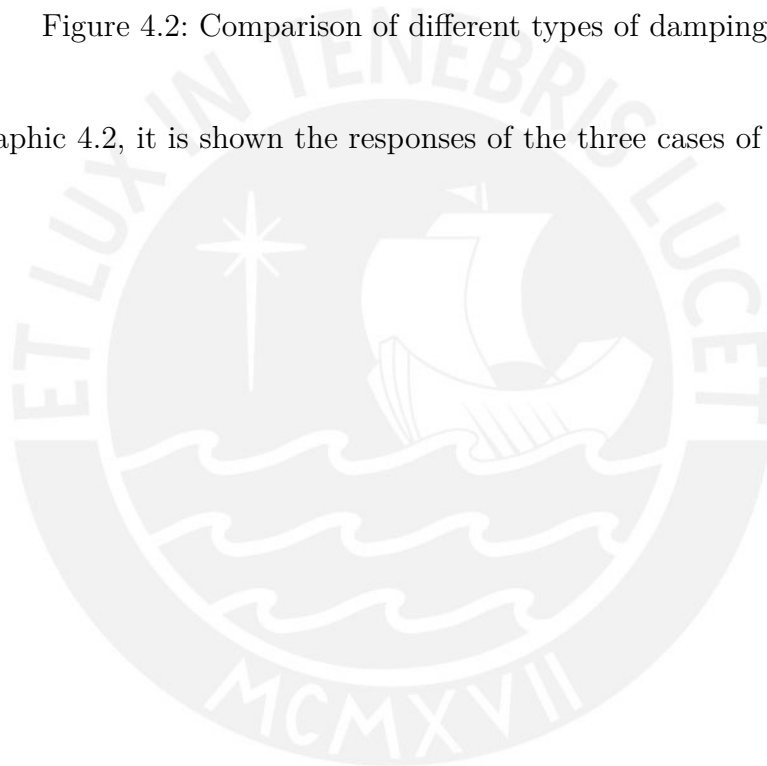
Figure 4.2: Comparison of different types of damping [RY95]

In the graphic 4.2, it is shown the responses of the three cases of free vibrations with damping.

4.2 Spring Design

Springs are mechanical elements with elastic properties which store energy when they suffer longitudinal deformation and regain its initial length. They can be used for multiple applications where it is required to apply a force and then being returned as energy; e.g. vehicle suspension, connection cables, foldable chairs. Because of its importance in the industry, they have been thoroughly studied for development and manufacture taking into account the materials and the calculations necessary to comply with their work properly. They can be classified in many ways e.g as spring form (cylindrical helical, conical helical, spiral), shaped cross section (circular, square, rectangular) and the type of burden (compression, extension, torsion).

Spring's main importance is the ability to store energy. So, for its construction there should contains material with high Elastic Modulus (E). Depending of their applications, it could be also desired to store energy without excessive losses or to absorb energy as much as possible to avoid rebound [Chu10].
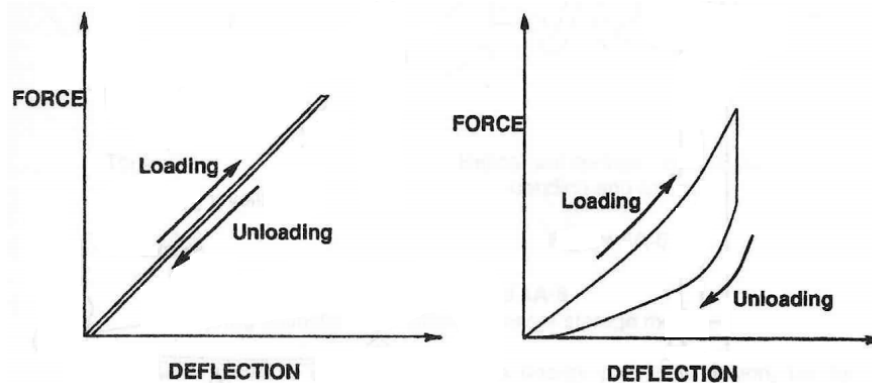
Figure 4.3: Graphs of response of Force vs Deflection for a spring with linear (left) and non-linear (right) behaviour[Chu10]

In figure (4.3), it can be seen that there are cases when springs have linear and non-linear characteristic. In the first case, where loading and unloading lines are straight (constant stiffness), the spring is composed of metal springs that have Low Hysteresis. In contrast, in the case where there is non-linear behaviour of the spring, it can be

made of material such as rubber or polymer [Chu10].

4.2.1 Stresses in Helical Spring

The figure 4.4 shows a compression coil spring, made with round wire, supporting an axial load. The parameter D indicates the mean diameter of the spring, while the parameter d indicates the wire diameter of the spring.
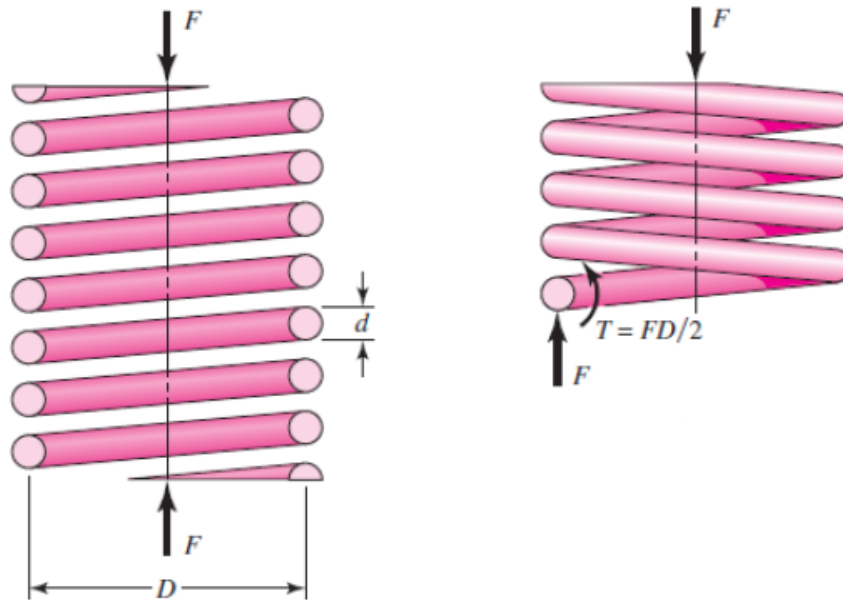
Figure 4.4: Helical Spring loaded axial [ML+13]

The maximum shear stress becomes from superposition of direct shear stress and torsional shear stress as it is seen in the next equation [SBM15]:

$$\tau_{max} = \frac{Tr}{J} + \frac{F}{A} \tag{4.17}$$

Where $\tau_{max} = \tau$, $T = FD/2$, $r = d/2$, $J = \pi d^4/32$, and $A = \pi d^2/4$. Finally, it is obtain the following:

$$\tau = \frac{8FD}{\pi d^3} + \frac{4F}{\pi d^2} \tag{4.18}$$

Then is defined C as spring index:

$$C = \frac{D}{d} \tag{4.19}$$

According to Design Handbook [Spr81], the value of C must be between 4 and 12. Low index could be difficult to manufacture and its process could trigger some small damages that could reduce life time. Otherwise, high index is difficult to handle, could tangle and may need a individual packaging [Spr81].

So, developing equation 4.18 and replacing spring index (C):

$$\tau = \frac{8FD}{\pi d^3} + \frac{8FdD}{2\pi d^3 D} = \frac{8FD}{\pi d^3}\left(1 + \frac{d}{2D}\right)$$

$$\tau = \frac{8FD}{\pi d^3}\left(\frac{2C+1}{2C}\right) = K_S \frac{8FD}{\pi d^3} \tag{4.20}$$

$$K_S = \left(\frac{2C+1}{2C}\right) \tag{4.21}$$

Where K_S is the *shear stress-correction factor*

4.2.2 Curvature effect

Because the wire in not straight, but curve, the curvature must be taken into consideration. It will increase the stress in the inner surface of the coil ([Cor15], [SBM15], [ML$^+$13]) for that reason, it is an important factor to be considered in spring design. This effect should be used for fatigue applications.

If the Curvature effect is added to shear stress-correction factor, the equation is obtained:

$$\tau = K\frac{8FD}{\pi d^3} \tag{4.22}$$

Where K can be replace for the next two forms:

$$K = K_B = \frac{4C + 2}{4C - 3} \tag{4.23}$$

$$K = K_W = \frac{4C - 1}{4C - 4} + \frac{0.615}{C} \tag{4.24}$$

K_B and K_W represents *Bergsträsser factor* and *Wahl factor* respectively. Literature indicates that the difference between these two factor is around 1%; however, Wahl factor is most used [SBM15].

4.2.3 Deflection of Helical Springs

When there is a load over compression springs, spring wire has a shear stress and torsional stress because load tries to twist the coils in relation to the axis. To determine the relation between the deflection and force applied on the spring, Castigliano's theorem is commonly used. It describes the strain energy for a helical spring produced by torsional and shear components [SBM15]. The strain energy in the spring is:

$$U = \frac{T^2 l}{2GJ} + \frac{F^2 l}{2AG} \tag{4.25}$$

Where $T = FD/2$ (Torque), $l = \pi DN$ (length of wire), $J = \pi d^4/32$ (Moment of inertia), $A = \pi d^4/4$ (Transversal area of spring). Then it results in:

$$U = \frac{4F^2 D^3 N}{d^4 G} + \frac{2F^2 DN}{d^2 G} \tag{4.26}$$

$N = N_a$ is number of active coils.

To determine the deflection, Castigliano's theorem is used:

$$\delta_i = \frac{\partial U}{\partial F_i} \tag{4.27}$$

Then:

$$\delta = \frac{8FD^3 N}{d^4 G} \left(1 + \frac{d^2}{2D^2}\right) = \frac{8FD^3 N}{d^4 G} \left(1 + \frac{1}{2C^2}\right) \tag{4.28}$$

The term $\left(1 + \frac{1}{2C^2}\right)$ can be approximated to zero when $4 < C < 12$

Then:

$$\delta \approx \frac{8FD^3N}{d^4G} \tag{4.29}$$

Finally, obtaining the spring rate:

$$k = \frac{F}{\delta} \approx \frac{Gd^4}{8D^3N} \tag{4.30}$$

4.2.4 Compression springs

Compression springs are used to support compressive stresses and shock. Therefore they reduce their volume when a force exerted on them, making them energy storage devices very efficient. According to its geometry, one can find multiple compression springs of different shapes: cylindrical coil springs, coil stamping, conical helical, bi-conical helical.

Compression springs have separate coils evenly. They are compressed when forces are applied at its ends, when this happens, its coils are equally close since they receive the same pressure resistance. Compression spring must never be deflected until its solid length because it would trigger a permanent deformation. Actually, it is suggest to do not deflect it too much because at the last 15% of its total deflection, the stiffness becomes non-linear due to there would be some active coils at the end of the spring which will close becoming them inactive.
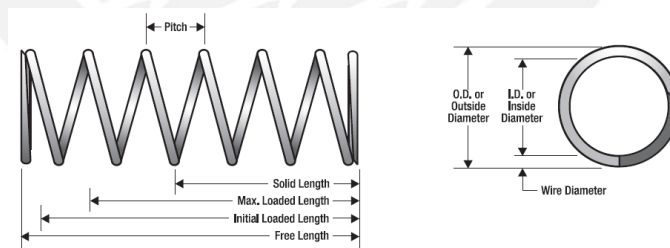
Figure 4.5: Compression spring [Cor15]

As it can be seen in figure 4.6, there are four typical types of end.
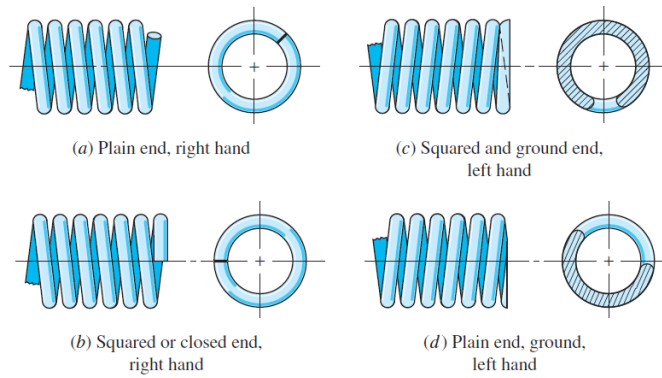
Figure 4.6: Types of ends of compression springs [SBM15]

| | | Type of Spring Ends | | |
| | | | | |
Term	Plain	Plain and Ground	Squared or Closed	Squared and Ground
End coils, N_e	0	1	2	2
Total coils, N_t	N_a	$N_a + 1$	$N_a + 2$	$N_a + 2$
Free length, L_0	$pN_a + d$	$p(N_a + 1)$	$pN_a + 3d$	$pN_a + 2d$
Solid length, L_s	$d(N_t + 1)$	dN_t	$d(N_t + 1)$	dN_t
Pitch, p	$(L_0 - d)/N_a$	$L_0/(N_a + 1)$	$(L_0 - 3d)/N_a$	$(L_0 - 2d)/N_a$

Figure 4.7: Formulas for Dimensional Characteristics of Compression springs [SBM15]

4.2.5 Stability

Spring must be studied for avoiding case of buckling when there is a large load. So, to verify that spring will not suffer buckling, the critical deflection should be calculated, and is given by:

$$y_{cr} = L_0 C'_1 \left[1 - \left(1 - \frac{C'_2}{\lambda_{cff}^2} \right)^{1/2} \right] \qquad (4.31)$$

y_{cr} corresponds to the deflection where instability starts [,]. λ_{cff} corresponds to effective slenderness ratio and is given by:

$$\lambda_{cff} = \frac{\alpha L_0}{D} \qquad (4.32)$$

The constants C'_1 and C'_2 are defined by:

$$C'_1 = \frac{E}{2\,(E - G)}$$

$$C'_2 = \frac{2\pi^2\,(E - G)}{2G + E}$$

Absolute stability occurs when $\frac{C'_2}{\lambda_{eff}^2}$ is greater than unity [SBM15]. So, the next condition must be satisfied:

$$L_0 < \frac{\pi D}{\alpha}\left[\frac{2\,(E - G)}{2G + E}\right]^{1/2} \tag{4.33}$$

End Condition	Constant α
Spring supported between flat parallel surfaces (fixed ends)	0.5
One end supported by flat surface perpendicular to spring axis (fixed); other end pivoted (hinged)	0.707
Both ends pivoted (hinged)	1
One end clamped; other end free	2

Figure 4.8: End-condition constant α [SBM15]

In the case of steels, the condition would be:

$$L_0 < 2.63\frac{D}{\alpha} \tag{4.34}$$

4.2.6 Materials

Elasticity is a mechanical property of the objects to be deformed and regain its original shape once upon forces that cause it disappear. The basis of operation of the springs relies on the material properties, among them is the steel, which can undergo significant elastic deformation. Among the materials used to manufacture springs, carbon steels are used. To regain initial length of the spring, it is necessary that the material has a high elastic limit. It is important to note that the yield depends on the diameter of the wire, as long as the diameter is increased, the yield decreases. The springs in their

operation support alternative and repeated efforts, it is important that the steel to be used have a high resistance to fatigue [Chu10].

It is also important that in manufacturing, spring do not suffer surface decarburization since the peripheral portion of the spring is more fatigued, then its resistance would be lower and may result in spring break [Chu10]. Another important factor is the shear modulus. This factor characterizes the change in shape experimented by the material when is subjected to shear forces. For linear elastic materials such as used in compression springs, the shear modulus has the same value in all directions. It is calculated as follows:

$$G = \frac{E}{2\left(1+\nu\right)} \tag{4.35}$$

G: Shear modulus
E: Elasticity modulus
ν: Poisson's ratio (For steel $\nu \approx 0.3$)

Spring material can be examined for their tensile strength, which vary according to its wire diameter, so it is needed to be known. The processing of the material has also an effect on tensile strength. The next equation is useful to estimate the tensile strength by previously knowing the wire diameter to identify the constants involve in the equation:

$$S_{ut} = \frac{A}{d^m} \tag{4.36}$$

Material	ASTM No.	Exponent m	Diameter, in	A, kpsi · in^m	Diameter, mm	A, MPa · mm^m	Relative Cost of Wire
Music wire*	A228	0.145	0.004–0.256	201	0.10–6.5	2211	2.6
OQ&T wire[†]	A229	0.187	0.020–0.500	147	0.5–12.7	1855	1.3
Hard-drawn wire[‡]	A227	0.190	0.028–0.500	140	0.7–12.7	1783	1.0
Chrome-vanadium wire[§]	A232	0.168	0.032–0.437	169	0.8–11.1	2005	3.1
Chrome-silicon wire[‖]	A401	0.108	0.063–0.375	202	1.6–9.5	1974	4.0
302 Stainless wire[#]	A313	0.146	0.013–0.10	169	0.3–2.5	1867	7.6–11
		0.263	0.10–0.20	128	2.5–5	2065	
		0.478	0.20–0.40	90	5–10	2911	
Phosphor-bronze wire**	B159	0	0.004–0.022	145	0.1–0.6	1000	8.0
		0.028	0.022–0.075	121	0.6–2	913	
		0.064	0.075–0.30	110	2–7.5	932	

Figure 4.9: Constants A and m to determine Minimum Tensile Strength [SBM15]

In figure 4.36, the table is useful to identify the constants A and m according to wire diameter.

Material	Elastic Limit, Percent of S_{ut}		Diameter d, in	E		G	
	Tension	Torsion		Mpsi	GPa	Mpsi	GPa
Music wire A228	65–75	45–60	<0.032	29.5	203.4	12.0	82.7
			0.033–0.063	29.0	200	11.85	81.7
			0.064–0.125	28.5	196.5	11.75	81.0
			>0.125	28.0	193	11.6	80.0
HD spring A227	60–70	45–55	<0.032	28.8	198.6	11.7	80.7
			0.033–0.063	28.7	197.9	11.6	80.0
			0.064–0.125	28.6	197.2	11.5	79.3
			>0.125	28.5	196.5	11.4	78.6
Oil tempered A239	85–90	45–50		28.5	196.5	11.2	77.2
Valve spring A230	85–90	50–60		29.5	203.4	11.2	77.2
Chrome-vanadium A231	88–93	65–75		29.5	203.4	11.2	77.2
A232	88–93			29.5	203.4	11.2	77.2
Chrome-silicon A401	85–93	65–75		29.5	203.4	11.2	77.2
Stainless steel							
A313*	65–75	45–55		28	193	10	69.0
17-7PH	75–80	55–60		29.5	208.4	11	75.8
414	65–70	42–55		29	200	11.2	77.2
420	65–75	45–55		29	200	11.2	77.2
431	72–76	50–55		30	206	11.5	79.3
Phosphor-bronze B159	75–80	45–50		15	103.4	6	41.4
Beryllium-copper B197	70	50		17	117.2	6.5	44.8
	75	50–55		19	131	7.3	50.3
Inconel alloy X-750	65–70	40–45		31	213.7	11.2	77.2

Figure 4.10: Mechanical properties of some springs [SBM15]

| Material | Maximum Percent of Tensile Strength | |
	Before Set Removed (includes K_W or K_B)	After Set Removed (includes K_s)
Music wire and cold-drawn carbon steel	45	60–70
Hardened and tempered carbon and low-alloy steel	50	65–75
Austenitic stainless steels	35	55–65
Nonferrous alloys	35	55–65

Figure 4.11: Mechanical properties of some springs [SBM15]

Music Wire 0.80-0.95C (ASTM A228)

Music wire is material mostly used for small springs because of it is the toughest material. This material has the higher tensile strength and also can withstand higher stresses with repeated loading than any other material. It can be found in diameters from 0.12 mm to 3mm[SBM15].

Oil-tempered wire 0.60-0.70C (ASTM A229)

This material is for general-purpose, and it is a good replacement when music wire is more expensive or when it is required a large size of spring. However, it is not recommended for uses of shock or impact loading. It is available in diameters from 3 mm to 12 mm [SBM15].

Hard-drawn wire 0.60-0.70C (ASTM A227-47)

It is the cheapest option for general-purpose spring steel. It should be only used when it is not required a long life, accuracy or deflection. It is available in diameters from 0.8 mm to 12 mm [SBM15].

Chrome-vanadium (ASTM A231-41)

It is the most popular alloy for conditions with higher stresses and when it is needed to work under fatigue and long endurance. It is also used for shock or impact loading. Available in annealed or pre-tempered sizes 0.8 mm to 12 mm in diameter [SBM15].

Chrome-silicon (ASTM A402)

This material is ideal for highly stressed springs which require long life and are intended

for shock loading. Available wire from 0.8 mm to 12 mm [SBM15].

4.2.7 Design for static service

For a design, a recommended number of active coils is $3 \leq N_a \leq 15$. It is worth to remind that to keep linearity, it is necessary that active coils do not gradually touch. Although ideally, helical spring force-deflection is linear, in practice, it is nearly so. However, not at each end of the curve of force-deflection [SBM15]. The spring is not able to reproduce a force for small deflection. Also, when it is near to closure, it lose its linearity because the pitch of spring is not accurately the same and produce touching of active coils under higher deformations. For this reason, it is desired that designer must confine the 75% of the curve between the spring without load ($F = 0$) and loading spring to closure ($F = F_s$) as the maximum deformation of the spring. Therefore, the maximum force endured for the spring should be $F_{max} \leq \frac{7}{8}F_s$. The ξ is defined as fractional overrun to closure and it is defined by:

$$F_s = (1 + \xi) F_{max} \tag{4.37}$$

Then:

$$F_s = (1 + \xi) F_{max} = (1 + \xi) \left(\frac{7}{8}\right) F_s \tag{4.38}$$

To solve the equation, ξ must be 1/7. So $\xi = \frac{1}{7} = 0.143 \approx 0.15$. Finally, it is recommended that $\xi \geq 0.15$.

The design conditions the be considered are the followings:

$$4 \leq C \leq 12$$

$$3 \leq N_a \leq 15$$

$$\xi \geq 0.15$$

$$n_s \geq 1.2$$

The safety factor to avoid closure is n_s For designing a helical coil compression spring, a design strategy suggested by SHIGLEY [SBM15] advise to make a priori decision

regarding the material of steel and consequently select the diameter of wire d. With decisions made before, it is possible to calculate the parameters: d, D, C, OD, ID, N_a, L_s, L_0, $(L_0)_{cr}$, n_s. It is required to use the material and wire size with the higher figure of merit, i.e. the best performance or efficiency. The figure 4.12 follows a strategy for designing a helical coil compression spring according to its application.
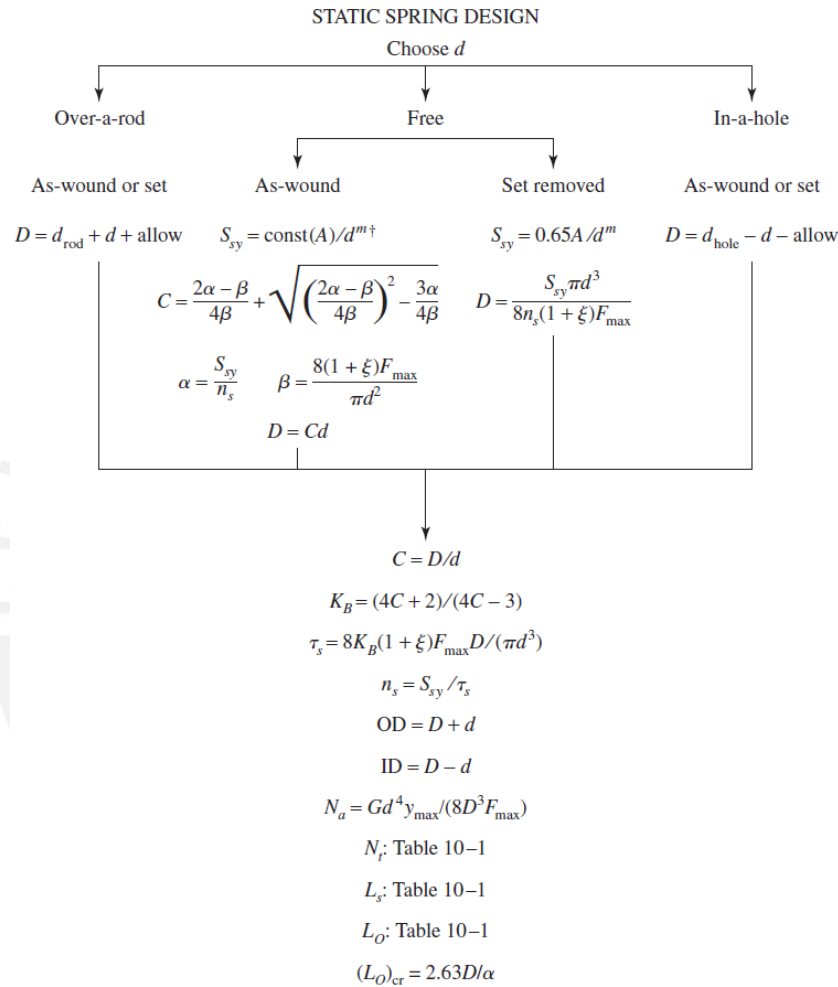

Figure 4.12: Design of helical coil compression spring for static loading [SBM15]

4.2.8 Critical frequency of Helical Springs

There are some applications that require helical coil compression spring for working with fast motion loading. Therefore, designer must assure that physical dimensions of

the spring are not able to get close to natural vibratory frequency, because it might produce resonance, triggering damaging stresses, given that internal damping in the spring are quite low [SBM15]. The equation that describes the translational vibration of a spring located between two parallel plate is given by:

$$\frac{\partial^2 u}{\partial x^2} = \frac{W}{kgl^2}\frac{\partial^2 u}{\partial t^2} \qquad (4.39)$$

Where: k: spring rate

g: acceleration of gravity

l: length of spring

W: weight of spring

x: coordinate along length of spring u: motion of any particle at distance x

The natural frequencies of a spring that is placed between two parallel plates can be obtained from the following equation:

$$\omega = m\pi\sqrt{\frac{kg}{W}} \qquad m = 1, 2, 3, \dots\dots \qquad (4.40)$$

The fundamental frequency is obtained with $m = 1$. Commonly, the frequency is interested in cycles per second, so the equation 4.41 determine it in hertz.

$$f = \frac{1}{2}\sqrt{\frac{kg}{W}} \qquad (4.41)$$

The equation to determine the weight of the operating part of the spring is given by the following:

$$W = AL\gamma = \frac{\pi d^2}{4}\left(\pi D N_a\right)(\gamma)\, g = \frac{\pi^2 d^2 D N_a \gamma}{4} g \qquad (4.42)$$

In equation 4.42, γ corresponds to specific weight or specific density ($steel = 7850\frac{kg}{m^3}$). It is used when calculations are in metric system, otherwise $\gamma = 0.284 lb/in$.

The fundamental critical frequency must be greater than frequency of force motion by 15 or 20 times. It is for avoidance of resonance with the harmonics. In case the design does not satisfy that conditions, it should be redesign to increase k and W.

4.2.9 Fatigue loading of Helical Compression Springs

Mostly, springs must be designed for working in high number of cycles, which can go from thousands to millions. For improve the mechanical properties of a spring, it can be treated by a process of shot peening. This process can increase the fatigue strength until 20% or more. According to SHIGLEY, the best data for about the torsional endurance limits of spring steels are provided by Zimmerli. Zimmerli figured out that size, material and tensile strength has no effect on endurance limits of springs steels when their sizes are under 10 mm. SHIGLEY observed that endurance limits increases with high tensile strengths[SBM15]. The endurance strength components for infinite life for unpeened and peened spring are:

Unpeened:

$$S_{sa} = 241 \quad MPa \quad (35 \quad kpsi) \qquad S_{sm} = 379 \quad MPa \quad (55 \quad kpsi) \tag{4.43}$$

Peened:

$$S_{sa} = 398 \quad MPa \quad (57.5 \quad kpsi) \qquad S_{sm} = 534 \quad MPa \quad (77.5 \quad kpsi) \tag{4.44}$$

$$S_{se} = \frac{S_{sa}}{1 - \left(\frac{S_{sm}}{S_{su}}\right)^2} \tag{4.45}$$

$$S_{se} = \frac{S_{sa}}{1 - \frac{S_{sm}}{S_{su}}} \tag{4.46}$$

Joerres, a member of Associated Spring-Barnes Group, recommends the Goodman relation for pulsation torsion [SBM15]. From Goodman diagram, Joerres uses:

$$S_{su} = 0.67 S_{ut} \tag{4.47}$$

Helical springs are never used as compression and extension, just have one of both applications. Usually, spring withstand a pre-loading.
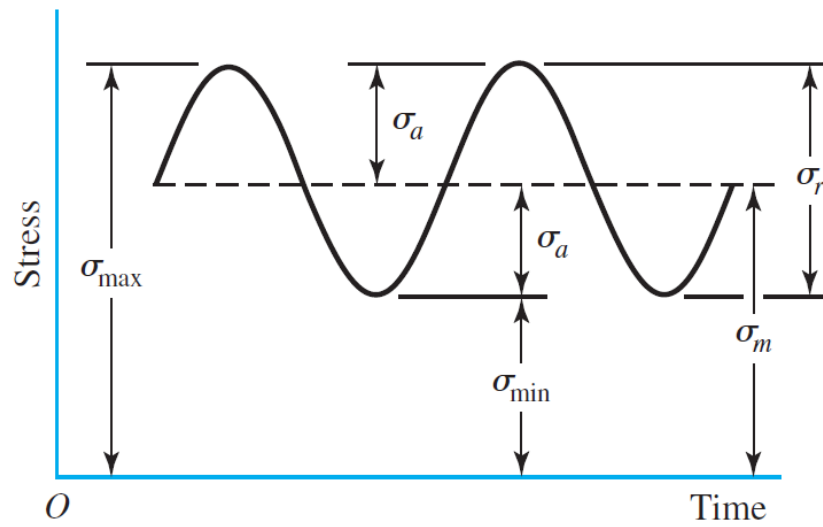
Figure 4.13: Sinusoidal fluctuating stress [SBM15]

Thus, from graph above, alternating and midrange component of forces are the followings:

$$F_a = \frac{F_{max} - F_{min}}{2} \tag{4.48}$$

$$F_m = \frac{F_{max} + F_{min}}{2} \tag{4.49}$$

Then, the shear stress amplitude and midrange shear stress are given by the equations:

$$\tau_a = K_B \frac{8F_a D}{\pi d^3} \tag{4.50}$$

$$\tau_m = K_B \frac{8F_m D}{\pi d^3} \tag{4.51}$$

5 Mechanical modeling

5.1 Description of the 1DoF model

The aim of this research is not to represent exactly all the components involved in the Follicle-sinus complex, but to exploit the internal behaviour for applications with tunable compliance. The model used for this research is the represented in figure 6.1. It contents a cylindrical rod with a pivot on a point of this. The lower end of the rod is joined with a system damper-spring. The reason why the model used has the system damper-spring in the lower end and not on other sides of the rod, it is because it represents an equivalent of a distribution of dampers and spring in a single one system.

This equivalent representation will change the values of proposed models of other researches; however, the behaviour will be the same. Thus, it would allow us to study the effects of a variation of the stiffness, which is our main objective in this current thesis. Therefore, the model is described in the following equation:

$$J_o\ddot{\theta}_{(t)} = F_{(t)}\left(\frac{l}{2} - \frac{l}{a}\right)cos\theta_{(t)} + mg\left(\frac{l}{2} - \frac{l}{a}\right)sin\theta_{(t)} - k\frac{l^2}{a^2}sin\theta_{(t)}cos\theta_{(t)} - c\frac{l^2}{a^2}cos^2\theta_{(t)}\dot{\theta}_{(t)}$$

$$(5.1)$$

Equation 5.1 describes the relation among the angular position and the other parameters, represented as variables. Where J_o is the inertia moment regarding the pivot, m mass of rod, k stiffness of spring, c damper of the system, g acceleration due to gravity, l length of the rod, a fraction of the rod regarding the pivot, $\theta_{(t)}$ angular position of the rod respect to vertical axis and $f_{(t)}$ the perpendicular force applied on the center of the rod. Also, using Steiner Theorem the calculate inertia moment, it is obtained

the following:

$$J_o = \frac{ml^2}{12} + m\left(\frac{l}{2} - \frac{l}{a}\right)^2 \tag{5.2}$$

In this equation 5.1, and with the objective of making it easier to solve, the friction in the pivot is considered null.
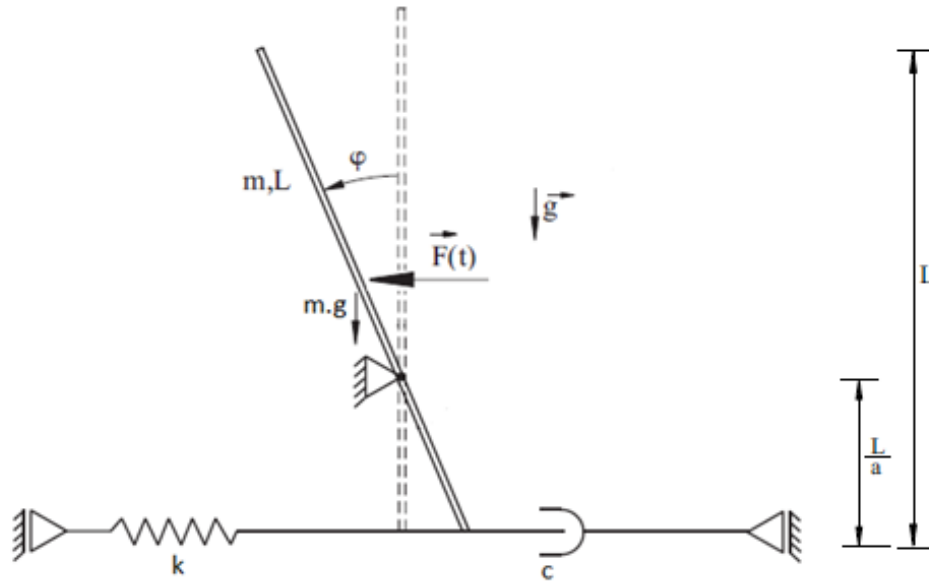

Figure 5.1: Model of 1DoF proposed for current thesis. Modify from [BSWZ13]

In order to reduce complexity of the equation, it is used an approximation of trigonometric ratios into angles:

$$sin\theta \approx \theta$$

$$cos\theta \approx 1$$

It is important to know that this approximation works properly until the angle of 15°. Therefore, it is expected to be some error when this angle increases more than 15°. However, this error will be also evaluated and compared with a multi-body simulation in the next chapters.

Then, the reduced equation obtain with approximation is represented in equation 5.3.

$$J_o\ddot{\theta}_{(t)} = f_{(t)}\left(\frac{l}{2} - \frac{l}{a}\right) + mg\left(\frac{l}{2} - \frac{l}{a}\right)\theta_{(t)} - k\frac{l^2}{a^2}\theta_{(t)} - c\frac{l^2}{a^2}\dot{\theta}_{(t)} \tag{5.3}$$

In the process of solving of the equation 5.3, that can be seen in CD attached to this document, it is obtained the new parameters $n_{1;2}$:

$$n_{1;2} = -\frac{cl^2}{2Ja^2} \pm \sqrt{\left(\frac{cl^2}{2Ja^2}\right)^2 - \frac{1}{J}\left[k\frac{l^2}{a^2} - mg\left(\frac{l}{2} - \frac{l}{a}\right)\right]} \tag{5.4}$$

And after applying LaPlace Transform to solve the equation, the response obtained is:

$$\theta_{(t)} = \frac{1}{J}\left(\frac{l}{2} - \frac{l}{a}\right)\int_0^t g(t-\sigma)f(\sigma)d\sigma + \theta_{(0)}\left[\frac{1}{n_1 - n_2}(n_1 e^{n_1 t} - n_2 e^{n_2 t})\right] + \left(\dot{\theta}_{(0)} + \frac{cl^2}{Ja^2}\theta_{(0)}\right)g(t) \tag{5.5}$$

Where:

$$g_{(t)} = \frac{1}{n_1 - n_2}(e^{n_1 t} - e^{n_2 t}) \tag{5.6}$$

5.2 Evaluation of spring as a compliant component

In the model proposed, there are three options to provide compliance to the system. The first one would be by tuning the stiffness of the spring. The second one, would be by tuning the damping of the damper. The third one, would be by implementing both before mentioned.

In this current thesis, the compliance of the actuator have been achieved for the first option, with a spring with tunable stiffness. In order to accomplish the variation of stiffness, the method used is the same of Jack Spring (seen in State of the art). The equation of the stiffness of a spring is given by:

$$k = \frac{Gd^4}{8D^3 N_a} \tag{5.7}$$

Where k is the stiffness of the spring, G is the Shear modulus or modulus of rigidity, d is wire diameter, D is Diameter of coil, and N_a is the number of active coils. Hence,

from equation 5.7, the stiffness could be change by varying the one or some of the other parameters. Mechanically, from all the parameters involved in equation 5.7, the easiest one to be changed is the number of active coils N_a. The variation of number of active coils can be done mechanically, it is required to have pre-defined the values of wire diameter and diameter of coils in order to design the mechanical components of the system with their dimensions. Thus, compression spring must be used because, unlike extension spring, it has a pitch between its coils that make it ideal for implementing a mechanical element to limit or extend the number of active coils. The modulus rigidity G is a material parameter itself, given by books or by the manufacturer of springs. Thus, the values of d and D must be analysed to select spring which could withstand the operation proposed. As it was explained in state of the art, in foveal whisking, rats contact surface of objects with a frequency until $25Hz$. For that reason, the maximum frequency of operation for this study would be $25Hz$.

$$f_{op} = 25Hz \tag{5.8}$$

Then, the critical frequency must be analysed. From spring design section in this document, and according to Shigley:

$$f = \frac{1}{2}\sqrt{\frac{kg}{W}} \tag{5.9}$$

And for recommendation of Shigley's book, the critical frequency should be greater than 15 or 20 times the maximum frequency of operation. For this research, it is used the mean between those:

$$f_{cr} = 17.5 f_{op} \tag{5.10}$$

Decomposing the stiffness k and weight W into basic parameters, it is obtained the following:

$$f_{cr} = \frac{1}{2}\sqrt{\frac{Gd^2 g}{2\pi^2 D^4 N_a{}^2 \gamma}} \tag{5.11}$$

Here, it is worth to mention that equation 5.11 corresponds to an equation applying values in English system, otherwise in metric system that acceleration due to gravity g might be omitted.
The material selected for this research is Music wire, because it has strong properties

with would make robust for fatigue loading. Modulus of rigidity can be given by a book or for previous research. However, manufacturer has its own value which is close to the usually quoted in books. For this thesis, the characteristics of spring will be selected from Century Spring Corporation. By working with calculations of springs of Century Spring, it was determined that accurate calculations are obtained working with English system, because the values given in metric system has only a decimal point so it is rounded to its closer decimal producing loss of precision. Consequently, all calculations will be made with English system, and posteriorly the mechanical elements will be designed in metric system. Empirically, it was calculated that for Century Spring Corporation, the music wire material has a modulus of rigidity about $11.5Mpsi$ which is closer to given by Shigley $12Mpsi$. For calculation, the one used will be $G = 11.5Mpsi$.

Then, replacing the values to obtain the relationship among d, D and N_a.

$$(17.5)(25) = \frac{1}{2}\sqrt{\frac{(11.5Mpsi)d^2(386)}{2\pi^2 D^4 N_a{}^2(0.284)}} \qquad (5.12)$$

$$\frac{D^4 N_a{}^2}{d^2} = 1038.7 \qquad (5.13)$$

From the catalogue of Century Spring Corporations, wire diameter and Coil diameter can be selected to determined the number of active coils necessary for withstanding $25Hz$. For this research, the values selected were $d = 0.038in$ and $D = 0.382in$. Then, the number of active coils should be:

$$N_a = 8.39 \approx 8.5 \quad turns \qquad (5.14)$$

Usually, to select a spring, the total number of coils are presented, so it is needed to know its value depending of the type of ends for the spring. For this purpose, it is required a closed and ground end, which would mean that the total number of coils should be:

$$N_t = N_a + 2 = 10.5 \qquad (5.15)$$

The compression spring that satisfy the characteristic required is Century Stock num-

ber 71335 (page 108 from catalogue of Century Spring [Cor15]). It owns the following dimensions and characteristic:

$$d = 0.038in \quad (1mm)$$

$$D = 0.382in \quad (9.7mm)$$

$$L_0 = 1.75in \quad (44.5mm)$$

$$k = 6.3 \quad Lb/in \quad (1.1N/mm)$$

$$Suggested \quad Maximum \quad Deflection = 1.1in \quad (28mm)$$

$$Suggested \quad Maximum \quad Load = 7lbs \quad (31N)$$

$$L_s = 0.40in \quad (10.1mm)$$

$$N_t = 10.5 \quad turns$$

To determine the pitch between the coils, we use the following equation:

$$p = \frac{(L_0 - 2d)}{N_a}$$

$$p = 0.197in \quad (5mm)$$

This value is important to know because it will determine the pitch of the actuator which will vary the number of active coils.

5.3 Multi-body model

In order to have a clearer idea of how this system would operate in reality, a multi-body simulation was implemented by designing mechanically the elements to achieve the tuning of active coils of the compression spring. The software SolidWorks appropriate the tools necessary to observe the design proposed and a sight of its operation. Besides, SolidWorks allow to analyse its responses with graphics. For construction of element, the dimensions will be in metric system. SolidWorks 2016 version has been employed since the computer where multi-body simulation was created has a Microsoft's Windows 10 operating system. Microsoft's Windows 10 has compatibility problems to apply SolidWorks Motion complement in SolidWorks' version before 2016.

As it was mentioned before, the basement of the design is inspired in operation of Jack Spring. Therefore, a motor is used to vary the number of active coils of the spring. The mechanical elements must satisfy the dimensions of the compression spring selected in the section before. It is worth to mention that the mechanical system must provide a lineal and rotational displacement for the element which limits the number of active coils. Also, because a spring can only operate as compression spring or extension spring, no both, it is required to use two compression springs to compensate the case of extension spring operation, as it can be seen in figure 6.2.
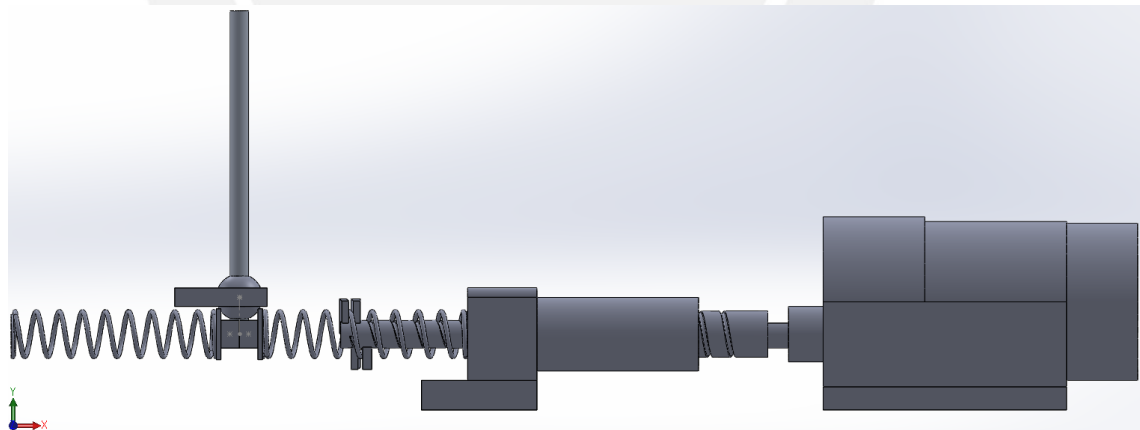

Figure 5.2: Frontal view of the multi-body model implemented in Solidworks 2016

5.3.1 Actuator

The actuator element used for generating motion is a motor, the velocity of changing of stiffness would depend on the angular velocity of motor. It is a variation of a coil per each turn (360°). For the design of the current thesis, the type of motor implemented in the multi-body simulation is a DC motor with encoder. It provides spins in both directions, and also could reach high velocities, which might be useful in applications that requires faster change of stiffness. The dimensions, in metric system, of a commercial DC motor (in CD attached to this document) were employed for building the body in SoliWorks. A DC motor has a cylindrical shape, so it required a basement for supporting it to keep it static. In figure 5.3, it can be seen the basement applied for supporting the DC motor. The motor is desired to have a fixed position, then the rotation of its axis should provide both lineal translation and rotation to vary the number of active coils of the spring.
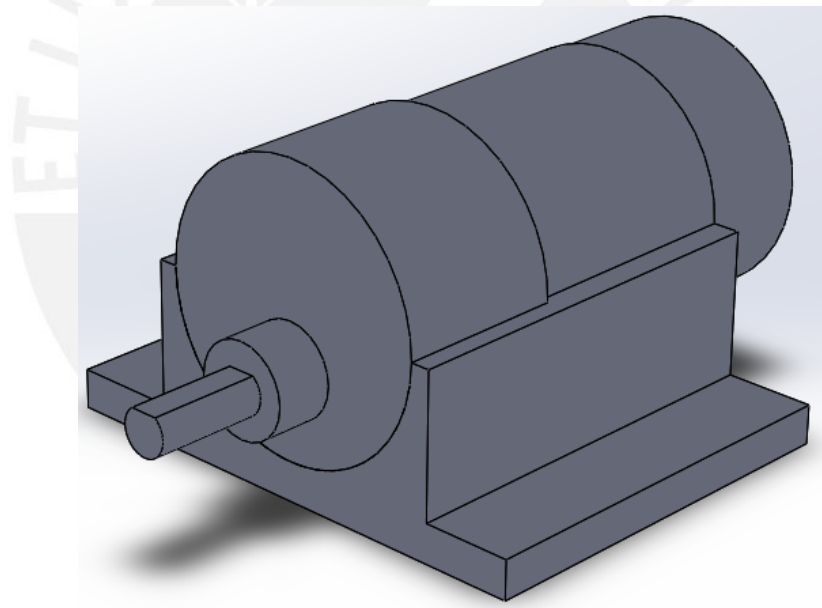

Figure 5.3: Isometric view of the motor

5.3.2 Couplings for limitation of active coils

To vary the number of active coils, it is necessary that a coupling could displace lineally with a pitch of $5mm$. In order to achieve this, the idea of worm screw is exploited to build elements that accomplish the required. For that reason, three elements were built with characteristic of screws. The first one should allow a coupling with the shaft of the DC motor, as can be seen in figure 5.4. Its external side has a shape of a bolt. This coupling only rotates, but do not displace lineally.

Then, the coupling for the motor must be connected to another element that should be displaced along of the spring (figure 5.5). This element has two sides. The first one has a shape like a nut to couple with the elements described before. The second one has a shape like a bolt which then will be couple to the support of the spring (figure 5.6) that has a nut shape and make possible the displacement.
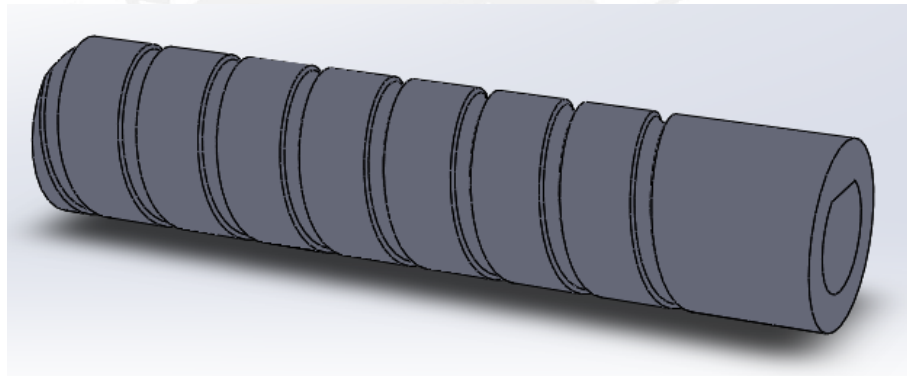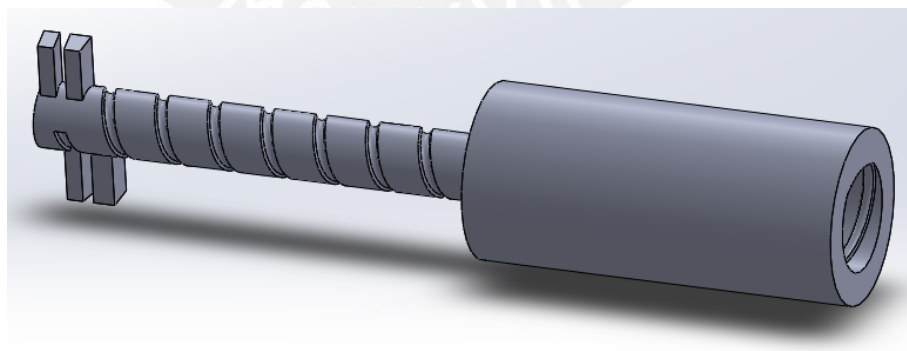

Figure 5.4: Coupling element for DC motor

Figure 5.5: Mechanical element with catcher to limit the coils of the compression spring

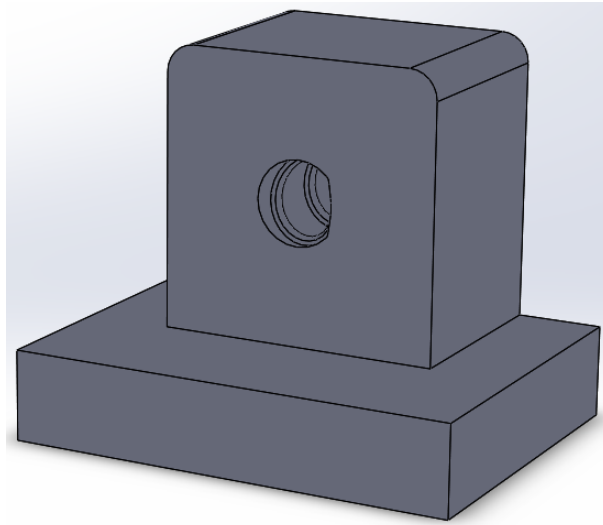*Master Thesis of Jorge Luis Ingaroca Quispe*

Figure 5.6: Support of the compression spring

The element which make possible the limitation of active coils is the one proposed in figure 5.5. It must catch a part of the active coils to convert the coils behind it to inactive coils. In the model, it can be seen that it has two catchers which have the enough space for the repose of wire coils. These catchers have a small angle of inclination. For calculating that angle is necessary to have the value of Diameter coil ($D = 9.7mm$) and the pitch ($p = 5mm$), as it can be observed in figure 5.7.
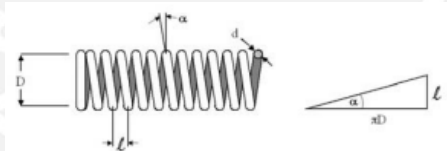

Figure 5.7: Geometry of a helical spring [HSH05]

$$\alpha = \tan^{-1}\left(\frac{p}{\pi D}\right) \tag{5.16}$$

$$\alpha = 9.3179° \tag{5.17}$$

The reason why it possesses two catchers is because just one would not be sufficient for a appropriate subjection of the coils. Since it might perform repeated loading, it

could induce vibrations in the spring if there is only one held point.

Thus, an mechanical element varies the number of active coils in the spring. However, it can not use all the active coils because the catchers has dimension that will no be possible to take the active coils from it starts, but a smaller number of coils. In figure 5.8, it is shown the dimension of the both catchers. The red point indicates the point where the number of active coils starts. Then, by adding the dimensions of the right side, we obtain:

$$Inactive\_length = 2.50mm + 1.74mm + 0.5mm \tag{5.18}$$

$$Inactive\_length = 4.74mm \tag{5.19}$$

Therefore, in reality, the active length of the compression spring would be:

$$Active\_length = p(N_a) - Inactive\_length = (5mm)(8.5) - 4.74 \tag{5.20}$$

$$Active\_length = 37.76 \tag{5.21}$$

Then the initial number of active coils would be:

$$N_a = \frac{(42.5 - Inactive\_length)(8.5)}{42.5} \tag{5.22}$$

$$N_a = 7.552 \quad turns \tag{5.23}$$

Thus, the initial stiffness of the spring must be calculated with 7.552 turns ($G = 11.55Mpsi = 76.924GPa$):

$$k = \frac{Gd^4}{8D^3N_a} = \frac{(76.934GPa)(0.0009652^4)}{8(0.0097^3)(7.552)} \tag{5.24}$$

$$k = 1.252N/mm = 1252N/m \tag{5.25}$$

According the number of active coils will be reducing, the stiffness will increase because

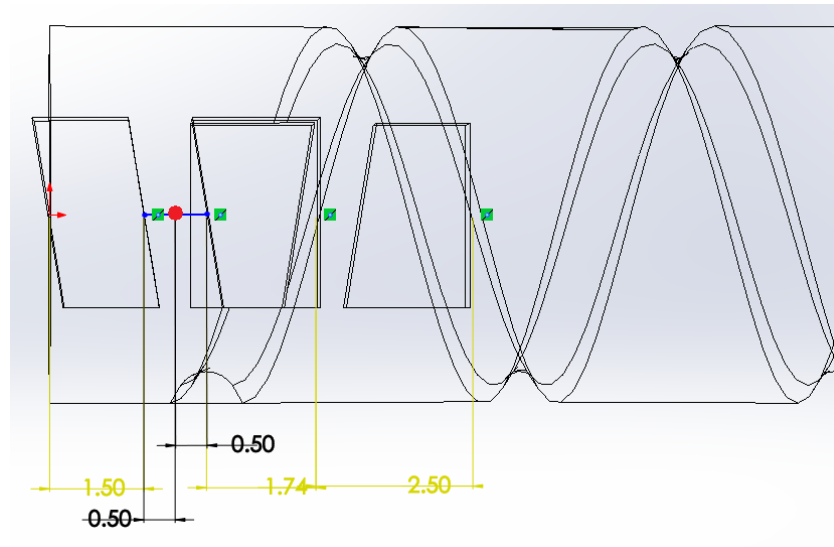Number of active coils is inversely proportional spring stiffness.

Figure 5.8: Design dimensions of the mechanical element that catches the wire coil

The compression spring, then, is built with the dimensions provided for manufacturer. The total number of coils is 10.5. However, it has closed and ground ends, so the number of active coils is 8.5. Previously, it was determined that the pitch has $5mm$. With these dimensions, the compression spring can be built as it is shown in figure 5.9.
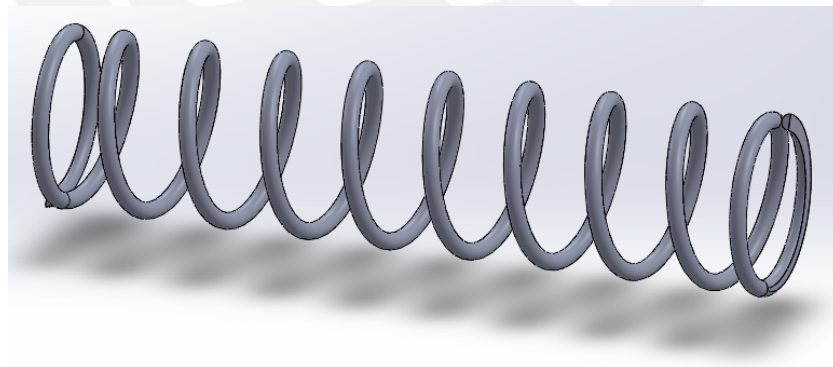

Figure 5.9: Compression spring built from Century Spring Corporation (Stock number 71335) with Closed and ground ends

5.3.3 Rigid body model

The system is inspired in the operation of a vibrissa, therefore to obtain a response which could give a response related to its real behaviour, an element similar to it is analysed. Vibrissa is a flexible sinus hairs; however, in this thesis it will be taken as a rigid body for practicality, since it is a first attempt to analyse viscoelastic properties of an actuator with tunable compliance. The aluminium cylindrical rod replace the vibrissa, so it has dimensions defined as $r = 2mm$ and $L = mm$, it has a pivot point which will be the eighth of its total length ($a = 8$). In figure 5.10
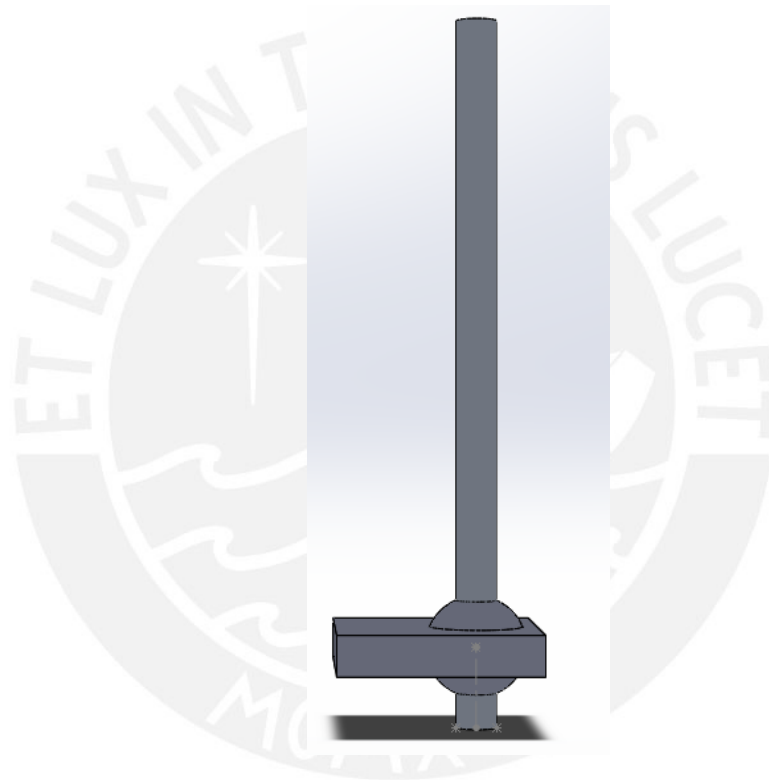

Figure 5.10: Rigid body to be analysed in motion. Rod with a pivot point.

The density of the aluminium is $Density = 2700kg/m^3$. Therefore, the mass of the rod would be $m = 0.0024kg$.

To provide an appropriate subjection of the spring, an element similar to a flat is fixed to the free end of the spring. Its importance endorse in transmitting correctly the force produced for the force to the spring, otherwise, it would not applied a longitudinal

deflection. For this, the element seen in figure 5.11, is proposed since it limit the movement in just one plane and provides the correct longitudinal deflection for the springs.
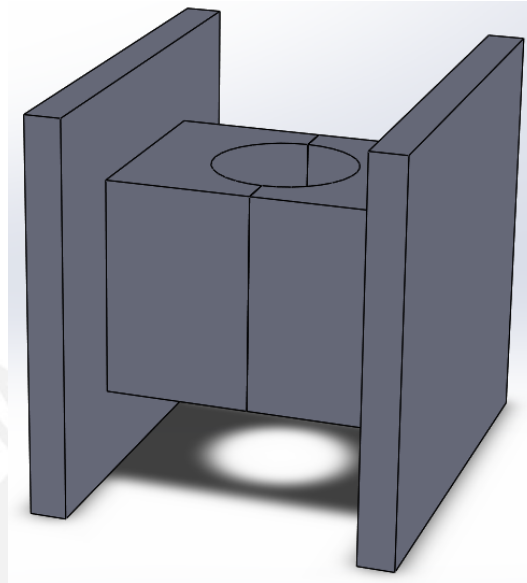

Figure 5.11: Flat supports fixed to the each spring end

6 Simulation of proposed system

6.1 Matlab simulation

In Chapter 5, it was described a model proposed for the system. For developing the equation that describes the system, an approximation of small angles were used, obtaining a response depending on the force that triggers the swinging of the rod and the initial conditions of the rod. It is important to observe how accurate this approximation is, so its response should be analyse and compare with the response of a Multi-body simulation, since the last owns more sources to simulate closer to reality. For that reason, Matlab software is employed, for describing the equations obtained and plot them. Once that dimensions of the elements of the systems are defined, it is possible to obtain the plots of the response for different cases. It is worth to remember that initial stiffness for the system is not the defined by the manufacturer in the catalogue because of the mechanical element used for catching the wire coil. It was previously calculated in Chapter 3 that initial stiffness is $k = 12552N/m$.

A system with vibrations needs a damper element to absorb the energy and stops the oscillations, otherwise it would oscillate without stopping. This current thesis focuses on the change of stiffness in a elastic element, in this case the spring. For that reason, the value of the damper will be fixed to $c = 5Ns/mm$.

The response of the system changes by adjusting the stiffness of the spring. To observe how it changes, the frequency of the system must be determined from the equation. Thus, it is part of the interest of this thesis to calculate how it varies depending on the value of the stiffness.
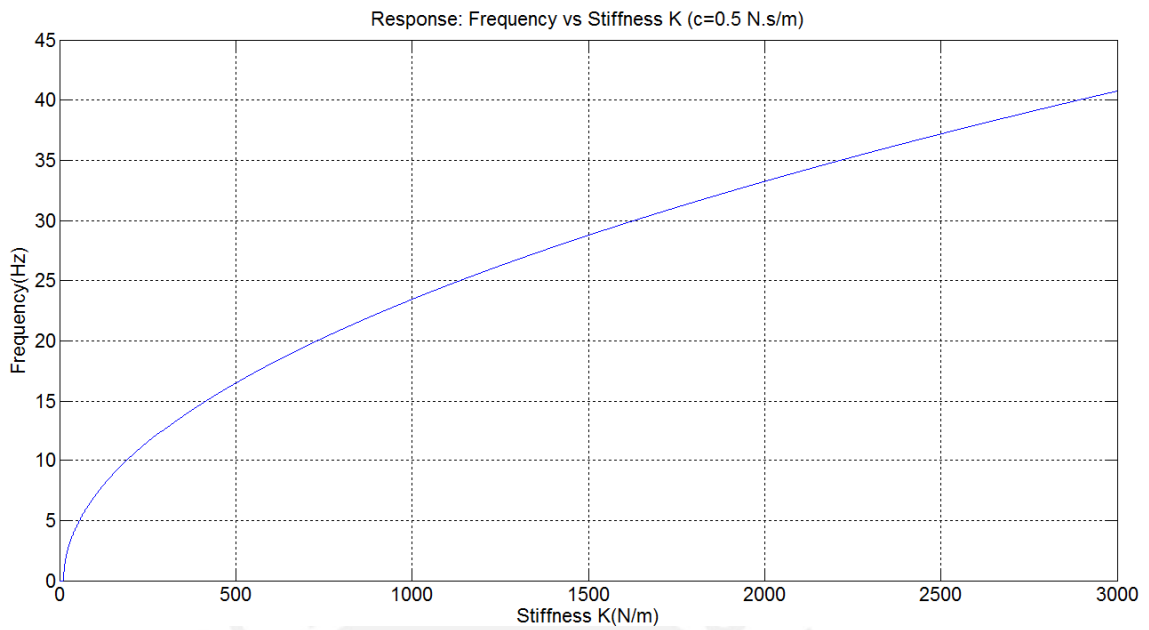
Figure 6.1: Frequency vs stiffness response with a damper of $c = 0.5Ns/m$

As it can be seen, the frequency increases regarding the increase of the stiffness. The initial stiffness is $k = 1255.2N/m$, and for that value, the frequency corresponds to $25Hz$ approximately. This value was our initial point of start to select the spring, so it satisfy the conditions of critical frequencies. Also, it is worth to mention that while reducing the number of active coils of the spring, the critical frequency of operation (view in Chapters before) will increase as well. Thus, the compression spring should have no problem for operating. For experiments, the force will be a rectangular pulse described by equation

$$f_{(t)} = F\left[u(t) - u(t - t_0)\right] \tag{6.1}$$

Therefore, the response of the angular position would be the following:

$$\theta_{(t)} = \frac{F\left(l - \frac{l}{a}\right)}{Jn_1n_2}\left[\frac{1}{n_2 - n_1}\left(n_1e^{n_2t} - n_2e^{n_1t}\right) + \frac{u(t - t_0)}{n_2 - n_1}\left(n_2e^{n_1(t-t_0)} - n_1e^{n_2(t-t_0)}\right)\right] +$$

$$\frac{F\left(l - \frac{l}{a}\right)}{Jn_1n_2}\left[1 - u(t - t_0)\right] + \theta_{(0)}\left[\frac{1}{n_1 - n_2}(n_1e^{n_1t} - n_2e^{n_2t})\right] + \left(\dot{\theta}_{(0)} + \frac{cl^2}{Ja^2}\theta_{(0)}\right)g_{(t)} \tag{6.2}$$

6.2 Solidworks simulation

Using the software SolidWorks, a mechanical demonstrator has been built for showing the dimensions and clarify the principle of operation. The complement SolidWorks Motion provides appropriate sources for a better Motion analysis of the system. Solid-Works Motion allows to introduce gravity to the system, to create dampers and springs, to measure parameters, to introduce lineal and rotational displacements, etc. The objective of the mechanical system is to limit the number of active coils of the compression spring. For this, the movement starts from the rotation of the shaft of the motor. This movement rotates the mechanical coupling ahead, and go on. This generates a transmission of movement until the mechanical coupling that catches the coils of the compression spring. The catcher has the same inclination of the coils of the spring, in order to couple precisely, i.e. the catcher and the wire coils are tangents. The mating relationships in the multi-body system fit properly; however, empirically, and error is observed when the mechanical couplings begin to rotate. It was found that catcher of the coupling and the wire coil are not exactly tangent, producing an alteration of the mating relationships. Then, another method must be applied in order to recreate the behaviour of the spring. For that reason, it is implemented an alternative way to recreate the behaviour of a the spring with a variation of their active coils.

As it is shown in figure 6.2, the main components which define the deflection and the length of the active region of the spring are selected. For measuring parameters such as distance and angular position, 'Results and Plots' tool is useful since it measures the parameter selected in all the simulation. Besides, these values are available to be employed in equations. The parameters required for these simulation are two. The first one, distance of the active length of the compression spring. And the second one, the deflection of the compression spring. For that reason, $D1$ measures the distance of the catcher from the axis Y. On another hand, $D2$ measures the deflection between the touch point of the rod and the beginning of the active coils. For offering a displacement of the coupling to simulate its rotation, Rotatory Motor is assigned to this in mode of Lineal Motor. Since the pitch of the compression spring is $5mm$, every step of $5mm$ would mean a turn of the motor and a variation of an active coil. The simulation incorporates a damper fixed to $c = 0.5Ns/m$ and in the same direction of
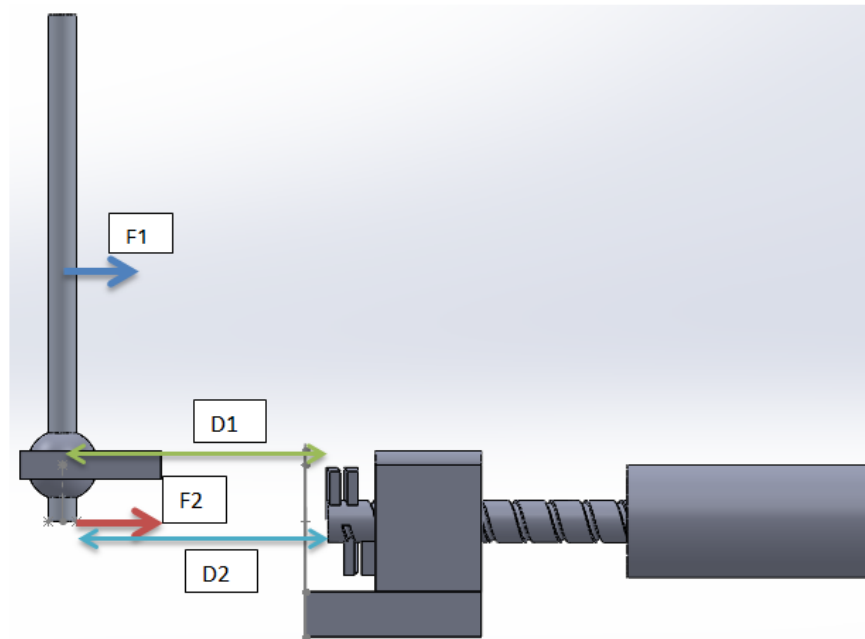
the compression spring.

Figure 6.2: View of the alternative method for simulating the behaviour of the system. $F1$ introduce external excitation and $F2$ the force due to compression spring deflection

For analysing the response of the system, many experiments are performed. To initialize the displacement of the angular position, two ways will be implemented: A perpendicular Force applied to the rod and variation of initial conditions of the rod, i.e. angular position and angular velocity. To observe variation of angular position. Results and Plots, from Solidworks motion, allow to measure in the process of simulation. The parameter selected is projection angle respect to Axis Z. After introducing deviation of angular position, the system stabilize in a short time. For that reason, simulation time is defined until one second. For improving the view of the plot, parameters of simulation are set. Thus, the number of frames per second, resolution of 3D contact and Precision are increased. The interface that SolidWorks provides to observe the response is not affordable for comparison with Matlab response. Then, results obtained by SolidWorks are exported as a CSV file. Posteriorly, this file is read by a Matlab command. and compared with its respective case.

6.3 Experiment results

6.3.1 Comparison between Mathematical model and Multi-body model

For comparing the results obtained in both models, some experiments were performed by changing the conditions for each one. In some cases, a perpendicular force is introduce to the rod in its inertia center. In other cases, initial angular position is modified. And also, there are cases were both, force and variation of angular position, are applied to the rod. Because, in this section is desired to analyse the response of the system described with approximation of small angles, the stiffness of the compression spring will be fixed to its initial value $k = 1255.2 N/m$

Experiment 1
For this experiment, the initial angular position is fixed in 10°. There are not external forces, so the rod tries to return to its stabilization point.
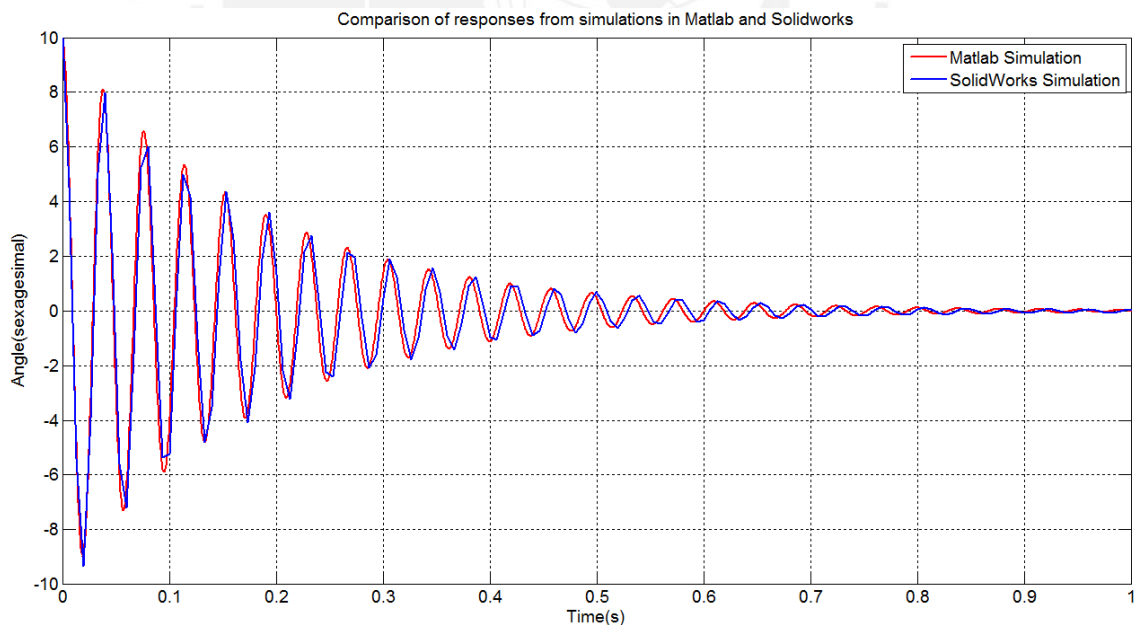

Figure 6.3: Comparison of responses of experiment 1 ($c = 0.5 Ns/m$)

Graphs from figure 6.3, have a similar response. The initial angular position is 10°, so the approximation of small angles works properly regarding amplitude and frequency.

Experiment 2

For this experiment, the rod is introduce with a initial angular position of 45°. No external forces are introduced in the model.
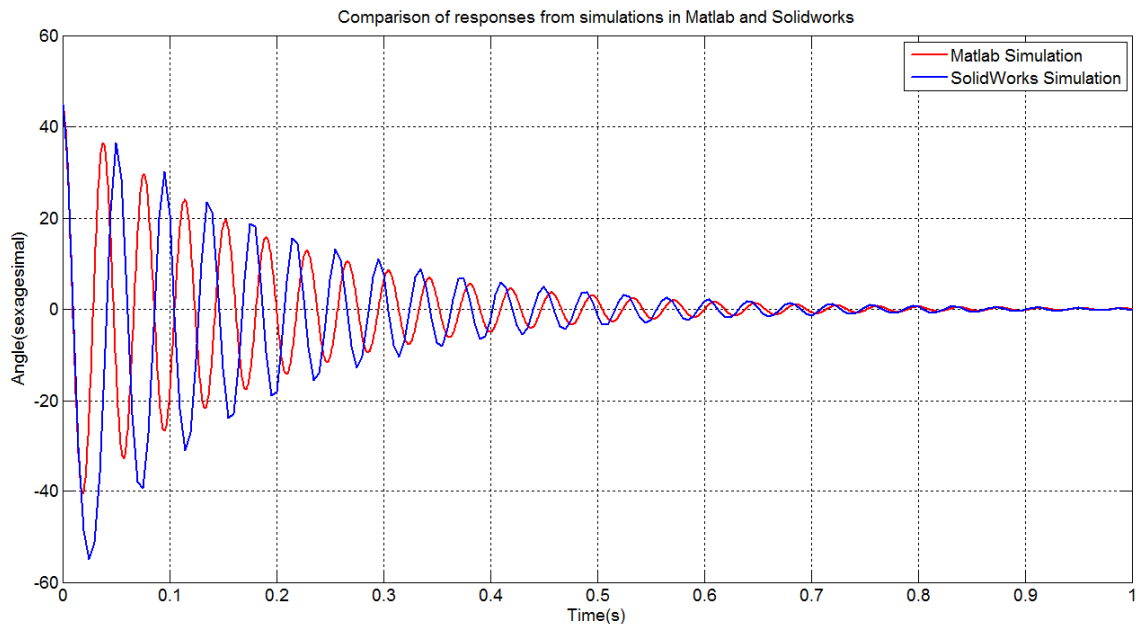

Figure 6.4: Comparison of responses of experiment 2 ($c = 0.5Ns/m$)

As it can be observed in figure 6.4, the response are not quite similar. The amplitude and frequency have almost the same value for both responses; however, there is an error because of the bigger deflection obtained in SolidWorks simulation which means more time for recovering its stabilization.

Experiment 3

For this experiment, the initial angular position is zero degrees, but a rectangular pulse force is introduced. The force introduced has a value of $F = 0.5N$ and $t_0 = 0.1s$, as

seen in the equation 6.3
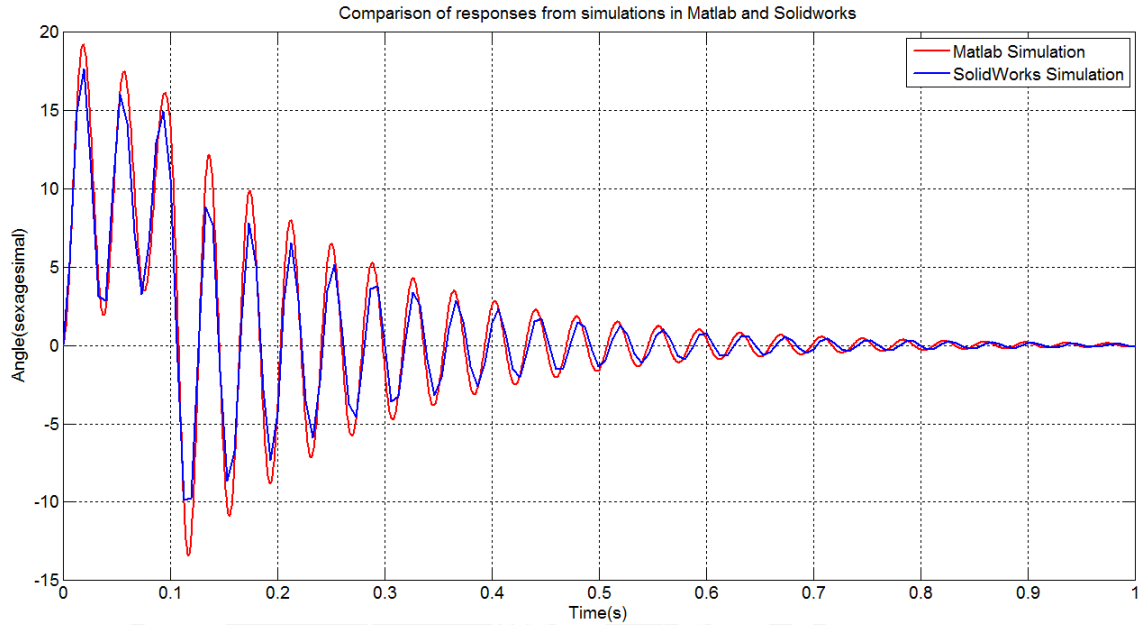
$$f_{(t)} = 0.5 \left[u(t) - u(t - 0.1) \right] \tag{6.3}$$

Figure 6.5: Comparison of responses of experiment 3 ($c = 0.5Ns/m$)

The responses obtained are quite similar. The main difference is the amplitude. The SolidWorks simulation has less amplitude than the Matlab simulation. The difference of deviation is not so high.

Experiment 4

For Experiment 4, the initial position is zero degrees. As well as experiment 3, rectangular pulse force is introduced, but it has a higher value $F = 1.5N$ and duration $t_0 = 0.25s$ as seen in equation 6.4

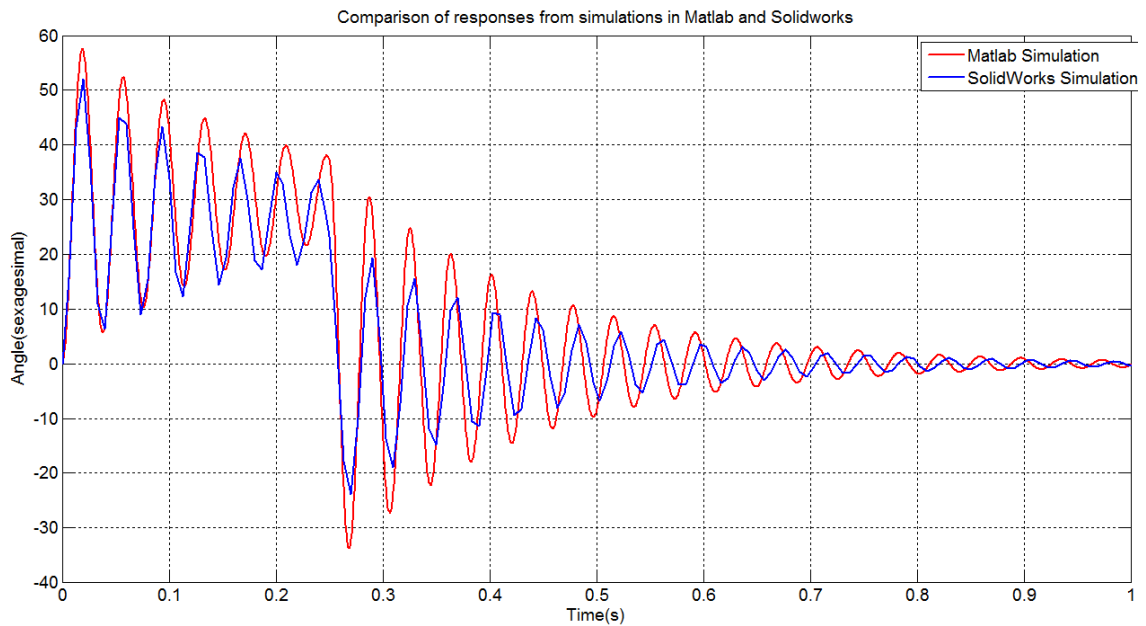$$f_{(t)} = 1.5 \left[u(t) - u(t - 0.25) \right] \tag{6.4}$$

Figure 6.6: Comparison of responses of experiment 4 ($c = 0.5Ns/m$)

As it is expected, in figure 6.6, the difference of amplitudes increases respect to experiment 3 because a greater deflection. Regarding to frequencies, they have a similar response.

Experiment 5

For this experiment, the rod has a initial angular position of 45°. Also, a force is introduce with a value of $F = 0.5N$ and a duration $0.2s$ (equation 6.5).

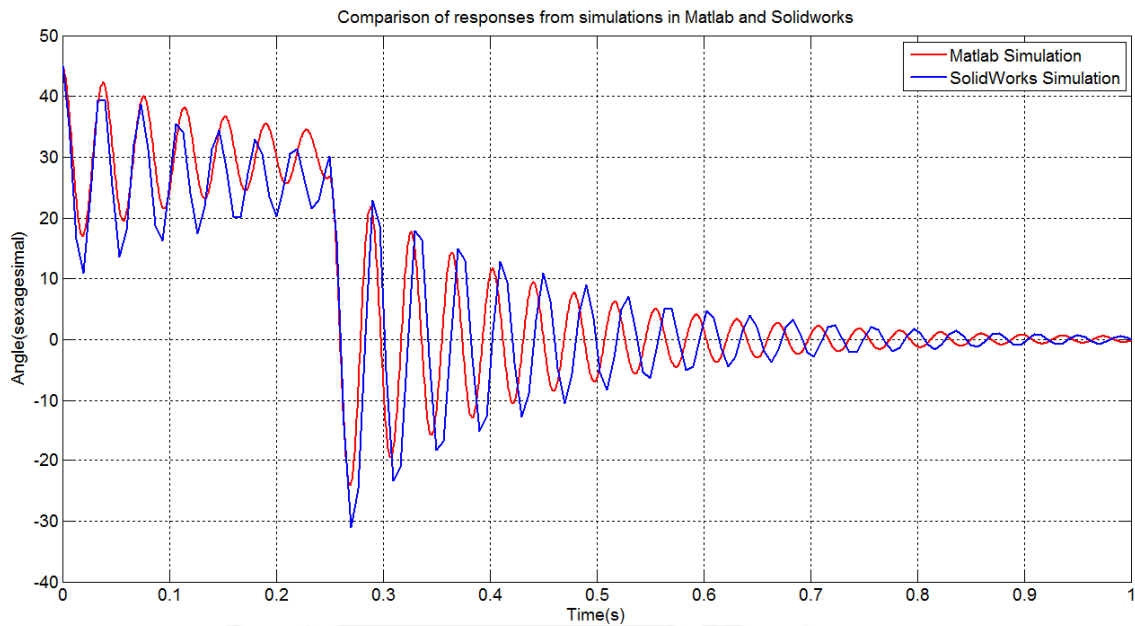$$f_{(t)} = 0.5\left[u(t) - u(t - 0.2)\right] \tag{6.5}$$

Figure 6.7: Comparison of responses of experiment 5 ($c = 0.5Ns/m$)

It is observed in figure 6.7 that rod oscillates while a force is applied on it. This is because the angular deviation is so high that force of the compression spring is increased enough to recover its stabilization despite of the force introduced. However, that force will be reducing while angular deviation increases, so the force applied is greater than force of the spring. Consequently, it increases the angular deviation and go on, until rectangular pulse force disappears. In this experiment, the amplitudes have not too much difference of values. Frequency is the same, but as seen in experiment 2, there is an error due to higher angular deviation in Solidworks simulation.

6.3.2 Analysis of the compliance

For this part of the simulation, the stiffness was tuned while the rod tries to return to its stabilization point. The rod is rotated with a certain angle, depending on the experiment. **Experiment 1**

For this experiment, the initial angular position is fixed in $10°$. There are not external forces, so the rod tries to return to its stabilization point. At the $time = 0.1s$ the motor started to rotate at a speed of $10rsps$ or $600rpm$ until $time = 0.2s$.
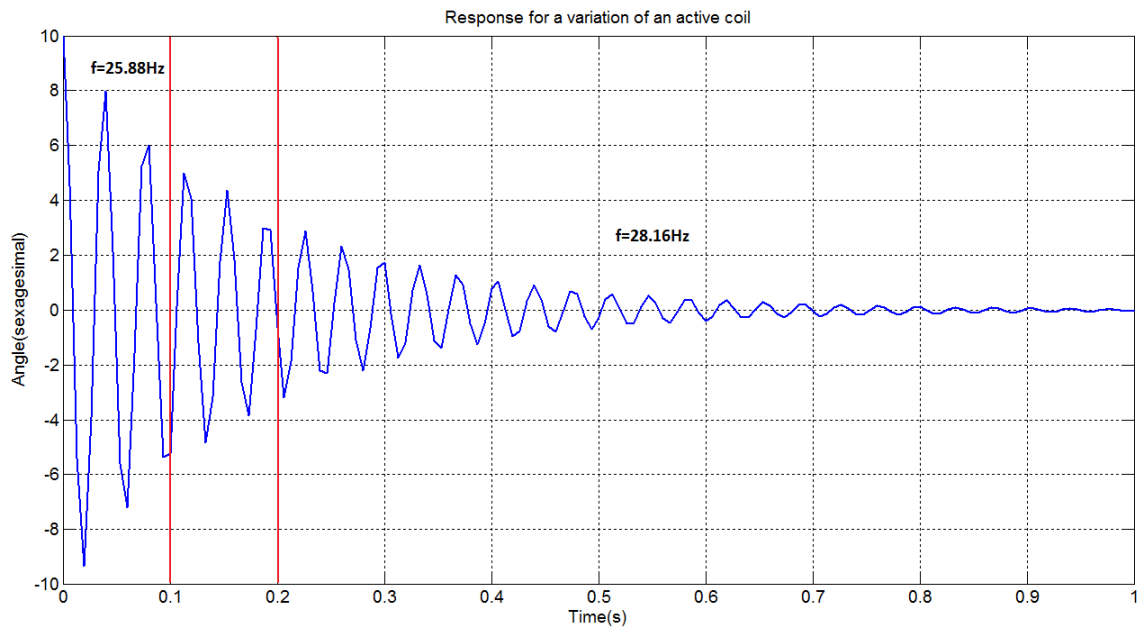

Figure 6.8: SolidWorks' response for experiment 1 ($c = 0.5Ns/m$)

As it can be seen in figure 6.8, the initial frequency is $f = 25.88Hz$ until the rotation starts. Later, after a transition state while motor stops, the frequency is increased until $f = 28.16Hz$. Because the rotation speed is $10rsps$, for a variation of time of $\Delta t = 0.1s$ the linear displacement would be $5mm$. It means that a complete active coil is decreased.

Experiment 2

For this experiment, the rod is introduce with a initial angular position of $45°$. No

external forces are introduced in the model. In this experiment, the motor start to rotate at $time = 0.1s$ until $time = 0.3s$ with the same speed of $10rps$
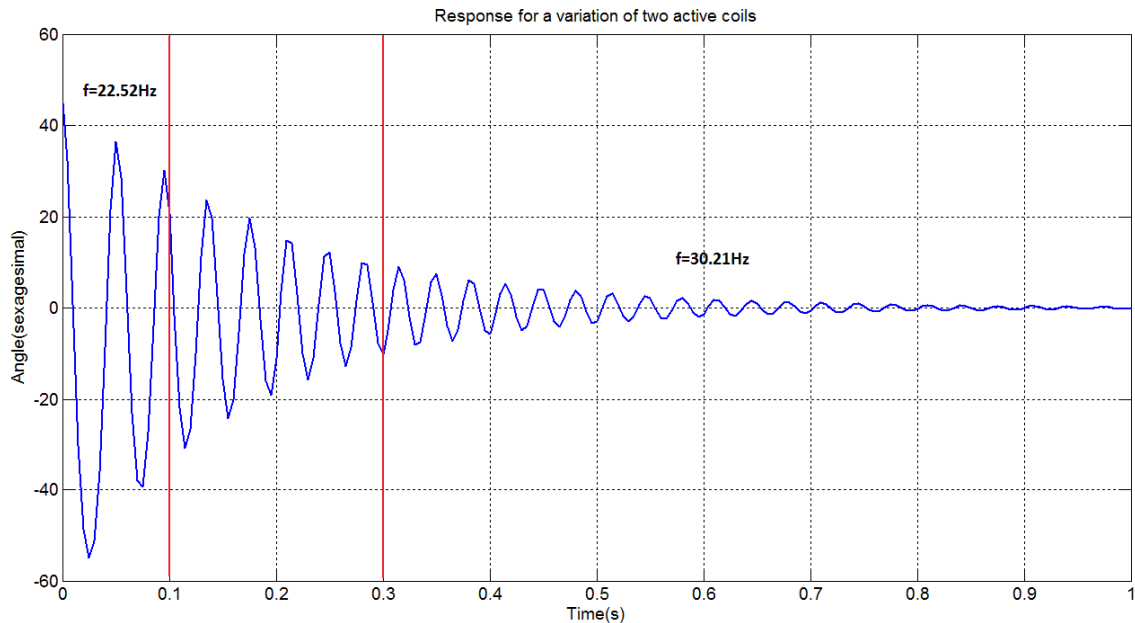

Figure 6.9: SolidWorks' response for experiment 1 $(c = 0.5Ns/m)$

From figure 6.9, it can be observed that frequency increases from $time = 0.1s$ when motor starts to rotate with a speed of $10rps$ until $time = 0.3s$. It means a displacement of $10mm$ which would also mean a decrease of two active coils.

7 Conclusions

Software for Multi-body simulation, as SolidWorks for this thesis, could have problems in simulation due to its own limitation. For instance, the conflict of mates between elements. Even when elements might have the same dimension to be mated, some movements generate conflicts such as rotation. Nevertheless, it is possible to apply sources for describing the behaviour as made in this work.

The comparison of the models developed in this current thesis indicates that they have characteristics quite similar, even for angular deviation greater than $15°$. That is the value limit where system is supposed to have greater errors. As it was observed, the approximated response works properly for a maximum deviation of $45°$.

By tuning the compliance of an actuator, the response of the system changes not only for frequencies, but for amplitudes as well because the value of stiffness is involved in the calculations of both parameters. However, obtaining the response of both parameters with a tunable stiffness will increase its complexity, so it would be required another strategy for calculations.

Bibliography

[Bed00]   BEDDARD, Frank E.: Vibrissae on the forepaws of mammals. In: *Nature* 62 (1900), S. 523

[BK03]   BERG, Rune W. ; KLEINFELD, David: Rhythmic whisking by rat: retraction as well as protraction of the vibrissae is under active muscular control. In: *Journal of neurophysiology* 89 (2003), Nr. 1, S. 104–117

[BSWZ13]   BEHN, Carsten ; SCHMITZ, Tonia ; WITTE, Hartmut ; ZIMMERMANN, Klaus: Animal vibrissae: modeling and adaptive control of bio-inspired sensors. In: *Advances in Computational Intelligence.* Springer, 2013, S. 159–170

[Car10]   CARL, Kathrin: *Technische Biologie des Tasthaar-Sinnessystems als Gestaltungsgrundlage fuer taktile stiftfuehrende Mechanosensoren*, Ilmenau, Techn. Univ., Diss., 2008, Diss., 2010

[Chu10]   CHURCHES, Alex: General notes on engineering Hardware. (2010)

[Cor15]   CORPORATION, Century S.: *Product catalog of Century Spring Corp.* 2015

[Dör82]   DÖRFL, Josef: The musculature of the mystacial vibrissae of the white mouse. In: *Journal of Anatomy* 135 (1982), Nr. Pt 1, S. 147

[EKM⁺02]   EBARA, Satomi ; KUMAMOTO, Kenzo ; MATSUURA, Tadao ; MAZURKIEWICZ, Joseph E. ; RICE, Frank L.: Similarities and differences in the innervation of mystacial vibrissal follicle–sinus complexes in the rat and cat: a confocal microscopic study. In: *Journal of Comparative Neurology* 449 (2002), Nr. 2, S. 103–119

[FAR95]   FUNDIN, BT ; ARVIDSSON, J ; RICE, FL: Innervation of nonmystacial

vibrissae in the adult rat. In: *Journal of Comparative Neurology* 357 (1995), Nr. 4, S. 501–512

[Fli14]   FLIEGNER, Caroline: *Entwicklung und anwendung eines verfahrens zur bestimmung des dynamischen verhaltens carpaler vibrissen von Ratten (Rattus norvegicus)*, Pontificia Universidad Católica del Perú, Escuela de Posgrado. Mención: Ingeniería Mecatrónica, Diss., 2014

[GDFM12]   GINTER, Carly C. ; DEWITT, Thomas J. ; FISH, Frank E. ; MARSHALL, Christopher D.: Fused traditional and geometric morphometrics demonstrate pinniped whisker diversity. In: *PloS one* 7 (2012), Nr. 4, S. e34481

[HBZK08]   HILL, Dan N. ; BERMEJO, Roberto ; ZEIGLER, H P. ; KLEINFELD, David: Biomechanics of the vibrissa motor plant in rat: rhythmic whisking consists of triphasic neuromuscular activity. In: *The Journal of Neuroscience* 28 (2008), Nr. 13, S. 3438–3455

[HSH05]   HOLLANDER, Kevin W. ; SUGAR, Thomas G. ; HERRING, Donald E.: Adjustable robotic tendon using a'jack spring'™. In: *Rehabilitation Robotics, 2005. ICORR 2005. 9th International Conference on* IEEE, 2005, S. 113–118

[HSV+09]   HAM, R v. ; SUGAR, Thomas G. ; VANDERBORGHT, Bram ; HOLLANDER, Kevin W. ; LEFEBER, Dirk: Compliant actuator designs. In: *Robotics & Automation Magazine, IEEE* 16 (2009), Nr. 3, S. 81–94

[HVN+14a] HELBIG, Thomas ; VOGES, Danja ; NIEDERSCHUH, Sandra ; SCHMIDT, Manuela ; WITTE, Hartmut: Characterizing the substrate contact of carpal vibrissae of rats during locomotion. In: *Biomimetic and Biohybrid Systems.* Springer, 2014, S. 399–401

[HVN+14b] HELBIG, Thomas ; VOGES, Danja ; NIEDERSCHUH, Sandra ; SCHMIDT, Manuela ; WITTE, Hartmut: *The Mechanics of Carpal Vibrissae of Rattus Norvegicus During Substrate Contact.* Universitätsbibliothek Ilmenau, 2014

[KKL+10]   KIM, J-N ; KOH, K-S ; LEE, Eun ; PARK, S-C ; SONG, W-C: The

morphology of the rat vibrissal follicle-sinus complex revealed by three-dimensional computer-aided reconstruction. In: *Cells Tissues Organs* 193 (2010), Nr. 3, S. 207–214

[MAKL06] MARSHALL, Christopher D. ; AMIN, Heidi ; KOVACS, Kit M. ; LY-DERSEN, Christian: Microstructure and innervation of the mystacial vibrissal follicle-sinus complex in bearded seals, Erignathus barbatus (Pinnipedia: Phocidae). In: *The Anatomical Record Part A: Discoveries in Molecular, Cellular, and Evolutionary Biology* 288 (2006), Nr. 1, S. 13–25

[MGR⁺04] MITCHINSON, Ben ; GURNEY, Kevin N. ; REDGRAVE, Peter ; MEL-HUISH, Chris ; PIPE, Anthony G. ; PEARSON, Martin ; GILHESPY, Ian ; PRESCOTT, Tony J.: Empirically inspired simulated electro-mechanical model of the rat mystacial follicle-sinus complex. In: *Proceedings of the Royal Society of London B: Biological Sciences* 271 (2004), Nr. 1556, S. 2509–2516

[ML⁺13] MARTÍNEZ LÓPEZ, Enrique u. a.: Cálculo de resortes helicoidales de compresión. (2013)

[NWS15] NIEDERSCHUH, Sandra J. ; WITTE, Hartmut ; SCHMIDT, Manuela: The role of vibrissal sensing in forelimb position control during travelling locomotion in the rat (Rattus norvegicus, Rodentia). In: *Zoology* 118 (2015), Nr. 1, S. 51–62

[RY95] RAO, Singiresu S. ; YAP, Fook F.: *Mechanical vibrations.* Bd. 4. Addison-Wesley New York, 1995

[SBM15] SHIGLEY, Joseph E. ; BUDYNAS, Richard G. ; MISCHKE, Charles R.: Mechanical engineering design. (2015)

[SCS05] SCHNEIDER, Axel ; CRUSE, Holk ; SCHMITZ, Josef: A biologically inspired active compliant joint using local positive velocity feedback (LPVF). In: *Systems, Man, and Cybernetics, Part B: Cybernetics, IEEE Transactions on* 35 (2005), Nr. 6, S. 1120–1130

[Spr81] SPRING, Associated: *Design handbook: engineering guide to spring*

design. Associated Spring, Barnes Group Inc., 1981

[SSWB11] SCHAEFER, Micha ; SCHMITZ, Tonia ; WILL, Christoph ; BEHN, Carsten: *Transversal Vibrations of Beams with Boundary Damping in the Context of Animal Vibrissae.* Universitätsbibliothek Ilmenau, 2011

[SWZ+14] SCHMIDT, Manuela ; WITTE, Hartmut ; ZIMMERMANN, Klaus ; NIEDERSCHUH, Sandra ; HELBIG, Thomas ; VOGES, Danja ; HUSUNG, Isabel ; VOLKOVA, Tatiana ; WILL, Christoph ; BEHN, Carsten u. a.: *Technical, non-visual characterization of substrate contact using carpal vibrissae as a biological model: an overview.* Universitätsbibliothek Ilmenau, 2014

[VHVVD+07] VAN HAM, Ronald ; VANDERBORGHT, Bram ; VAN DAMME, Michaël ; VERRELST, Björn ; LEFEBER, Dirk: MACCEPA, the mechanically adjustable compliance and controllable equilibrium position actuator: Design and implementation in a biped robot. In: *Robotics and Autonomous Systems* 55 (2007), Nr. 10, S. 761–768

[ZKRS04] ZINN, Michael ; KHATIB, Oussama ; ROTH, Bernard ; SALISBURY, J K.: Playing it safe [human-friendly robots]. In: *Robotics & Automation Magazine, IEEE* 11 (2004), Nr. 2, S. 12–21